<Review Article>Studies on Mechanical and Dielectric Relaxation Processes in Cellulose Derivatives

AUTHOR(S):

MOROOKA, Toshiro

Review Article

Studies on Mechanical and Dielectric Relaxation Processes in Cellulose Derivatives

Toshiro MOROOKA*

(Received September 1, 1987)

Contents

* Research Section of Wood Physics.

Introduction

Fossil resources including petroleum have been widely used as industrial raw materials for synthetic polymers and other compounds, as well as for energy sources. However, their future availability is considered to be limited and the countermeasures for the shortage of oil and natural gas are being investigated invarious fields. As an approach to this problem, further developments in the use of renewable resources are desired. Cellulose is a renewable resource which is produced in the largest quantities on the earth and is the basis of the variety of technical products such as fiber, paper, plastics, additives, etc. In most of such end-use applications of cellulose, it is necessary first to dissolve cellulose in some manner and then to re-form it from solution into the desired products. However, since the dissolving process of cellulose has been either cumbersome or expensive as compared to raw material, cellulose has not yet reached to its potential utility in many areas of application.

In recent years, new organic solvent systems for dissolving cellulose have been developed[1-3], partly including lithium chloride/dimethylacetamide (LiCl/DMA)[4], N-methylmorpholine-N-oxide (MMNO)[5], dinitrogen tetroxide/dimethylformamide (N_2O_4/DMF)[6], paraformaldehyde/dimethyl sulfoxide (PF/DMSO)[7], sulfar dioxide/diethylamine/DMSO (SO_2/DEA/DMSO)[8,9], and chloral/DMSO[10]. In applying these solvents, regeneration of cellulose for fiber production, co-regeneration of a mixed polymer systems for novel cellulose-polymer blends, liquid crystal formation of cellulose in solution etc. have been investigated[3].

The dissolving of cellulose can provide another mode of flexibility in preparing novel cellulose derivatives. While the derivatization of cellulose has chiefly been carried out so far as heterogeneous reaction, the use of above solvent systems opens a route to uniform cellulose derivatization which can produce new kinds of cellulose derivatives. For example, cellulose sulfate prepared in N_2O_4/DMSO medium is quite different in nature from those of sulfates prepared by heterogeneous means[11]. The reaction in MMNO gives acetyl and cyanoethyl cellulose which are soluble in water[12]. Chlorodeoxycellulose was obtained using chloral/DMSO system[13]. Tri-substituted product of benzylcellulose is produced by the reaction in SO_2/DEA/DMSO system[14]. In addition, methylation, carboxymethylation[15], silylation[16], and acetylation[17,18] in PF/DMSO medium has been reported.

In relation to the development of these new derivatives, it is predicted that the utilization of cellulose derivatives as plastic materials would increase still more in future. Therefore, systematic studies on their physical properties, especially viscoelastic properties are necessary. However, little work has been reported so far on the viscoelastic properties or molecular relaxation processes of cellulose

derivatives as compared with those of synthetic polymers.

The present studies are initiated to clarify systematically the relaxation processes for the cellulose derivatives in a molecular level. This is a three-part article. PART I describes relaxation processes in a series of conventional cellulose acylates. Although this series is one of the most important cellulose derivatives, little has been known for their relaxation mechanisms so far. The samples examined were prepared by trifluoro acetic anhydride-fatty acid esterification[12]. In contrast to this, PART II discusses relaxation processes for a series of acylated cellulose prepared by using PF/DMSO medium. Polymers in this series are substantially different in character from conventional series of the acylates. In PART III, application of PF/DMSO medium to cyanoethylation of cellulose is introduced. The resulting products are quite different in physical properties from the conventional cyanoethylcellulose, and are characterized on the basis of the result sobtained in PART II. All the samples examined are almost tri-substituted cellulose derivatives.

Two types of relaxation measurements are employed in this study. One is dynamic mechanical measurement. This is the most universal method of all, since it can determine a change in mobility of almost all sorts of motional units. The other is dielectric measurements. This can be performed over a wide frequency and temperature range, and it provides relatively complete information on molecular motions based on relaxation phenomena.

PART I Cellulose Acylates

1. Mechanical relaxation processess of cellulose acylates

Most attention to the dynamic mechanical properties of polymers in a series of cellulose acylates has centered around the acetate[20–23], since it is the most important member of the series in view of its industrial application. However, if we can understand characteristics of the relaxation processes of the wide variety of the acylates, it serves for constructing a fundamental view for both existing and potential cellulose derivatives. Klarman et al.[24] reported dynamic mechanical properties of the homologue of the acylates. However, the detected relaxation processes and their assignments appear to be unclear. This is partly because of the fact tht the samples examined were supplied by various companies, and thus they seem to be somewhat different in nature.

The present chapter describes dynamic mechanical properties of homologue of cellulose acylates from the propionate to the decanoate measured over a wide temperature range[25]. All the samples employd in this experiment are prepared by trifluoro acetic anhydride-fatty acid esterification, which is conisdered to be suitable

for this experiments, since it induces no notable cellulose degradation and results in pure and colorless products[26]. In the following, the dynamic mechanical properties for filmed specimens were measured with a direct reading viscoelastometer. Complex modulus and loss tangent were measured in the temperature range from −190°C to 200°C at four constant frequencies of 3.5, 11, 35, and 110 Hz. The programmed heating rate was about 1°C/min. The size of specimens was 0.2 mm thick × 2 mm wide × 4 cm long for measurements in the temperature range from −190°C to 30°C, and 1 mm thick ×2 mm wide × 2 cm long in the range from 30°C to 200°C.

1.1 Classification of the processes detected

The results of dynamic modulus E', loss modulus E'' and loss tangent $\tan\delta$ at 100 Hz as a function of temperature for cellulose butyrate are presented in Figure 1-1. With respect to E'', four relaxation processes are detected within the experimental frequency and temperature ranges, being labelled α_m, β_m, β'_m and γ_m processs in order of decreasing temperature at which they were detected.
These four processes were also observed for the valerate and the decanoate in the temperature range between −190°C and 150°C at 110 Hz. However, the γ_m process for the propionate and the β'_m process for the decanoate were not observed. On the contrary, a relaxation process, labelled γ'_m, for the propionate in the temperature range below −150°C was detected, which was not recognized for the other acylates. In the following, the relaxation mechanism for these α_m to γ_m' processes are

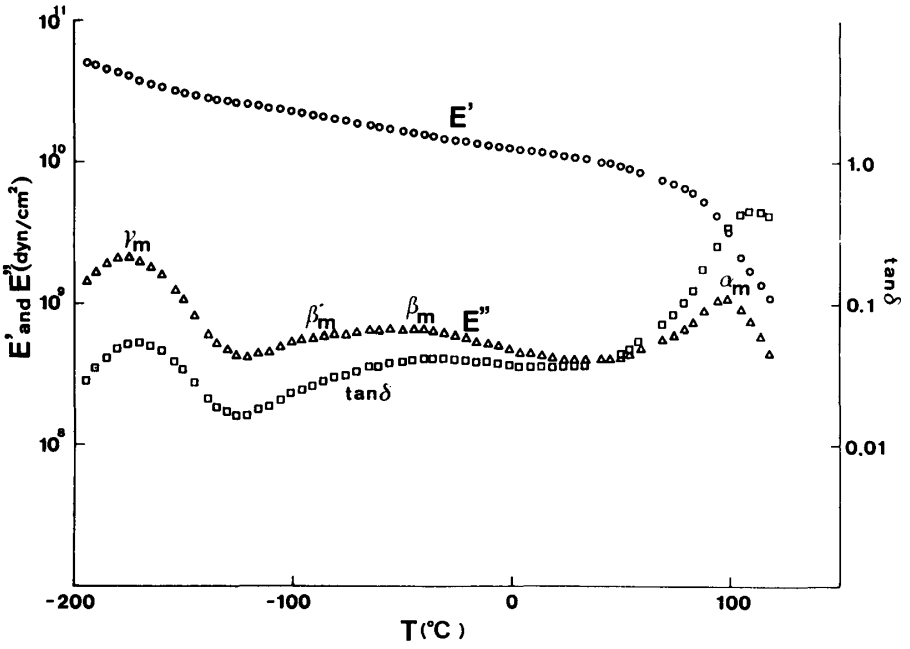

Fig. 1-1. Temperature dependence of dynamic modulus E', loss modulus E'', and loss tangent $\tan\delta$ at 110 Hz for cellulose butyrate.

discussed in sequence.

1.2 The α_m process

Figure 1-2 shows the changes in E' at 35 Hz above room temperature for the acylates from propionate to decanoate. In the temperature range of the α_m process, a remarkable drop in E' is recognized. Especially, that for the acylates from valerate to decanoate extends by three orders in magnitude. Furthermore, the maximum $\tan\delta$ values in the α_m process for all the acylats were nearly equal to unity. These facts mean that this process is related to the glass-rubber transition, and so the α_m process is assigned to a micro-Brownian motion of the main chain of the acylates. The apparant activation energy ΔE for the α_m process was 55 to 121 kcal/mol, which is of the order of the principal dispersion. The temperature locations of E'' maxima in the α_m process, which is considered to be almost equal to the glass transition points T_g, are denoted by arrows in Figure 1-2. The T_g for the acylates apparently shifts to lower temperature region with increasing the number of carbon n in the indroduced acyl group. This phenomenon can be interpreted as follows: the increase in the molecular size of non-polar n-alkyl groups causes decreased interaction of dipolar ester group, thus facilitating the chain backbone motion. The effect is similar to that produced by the additin of

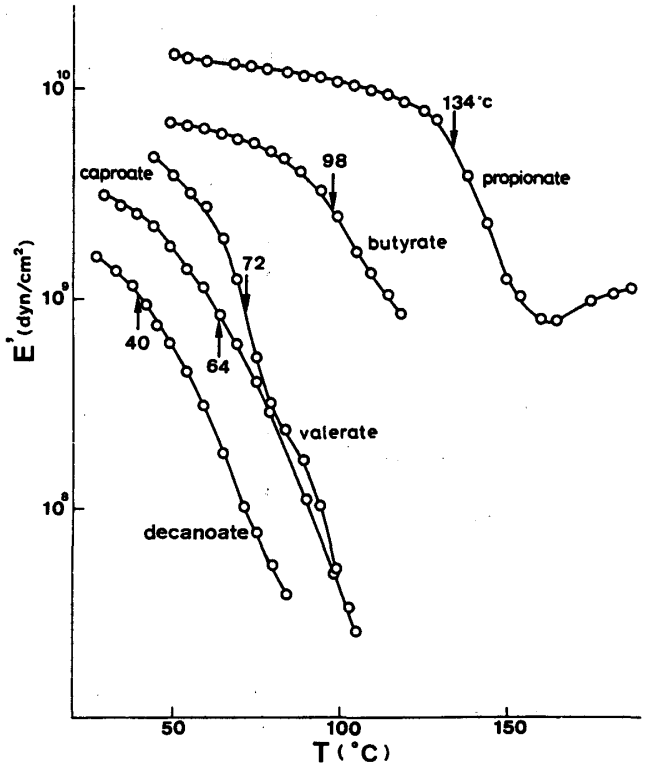

Fig. 1-2. Temperature dependence of dynamic modulus E' at 35 Hz for the acylates from propionate to decanoate.

plasticizer. However, the T_g seems to level off when n reached to about 6. This trend is similar to the results of the dielectric relaxation of cellulose acylates. However, this will be discussed later in Chapter 2. On the other hand, it is to be noted that the T_g for poly-*n*-alkyl methacrylates decreases continuously with increasing n, reaching -65°C for poly-*n*-dodecyl methacrylate[27]. This difference between cellulose acylates and poly-*n*-alkyl groups in the side chain, may be attributed to the different structure of the frame work; the former being bulkier than the latter. As is well known, the T_g of polymers is strongly dependent of their molecular weights. Therefore, the comparison of T_g for the acylates should be made for the samples having same order of molecular weight. All the samples prepared in this experiment gave molecular weight of the order of 10^5 (See 2.1), and so the results obtained are considered to be reasonable. In Figure 1-2, a rise in E' with temperature in the region just above T_g was recognized for the propionate. This rise in E' means the development of a structure which could support stress elastically, i.e. the crystallization of the sample[24,28]. This phenomenon was also observed for the other acylates.

1.3 The β_m process

The β_m process for the butyrate appeared in the temperature region at around -50°C in the E'' versus temperature curves shown in Figure 1-1. To compare the absorption magnitude in the β_m process among the acylates, tan δ curves should be used instead of E'' curves, because it is considered that tan δ corresponds to

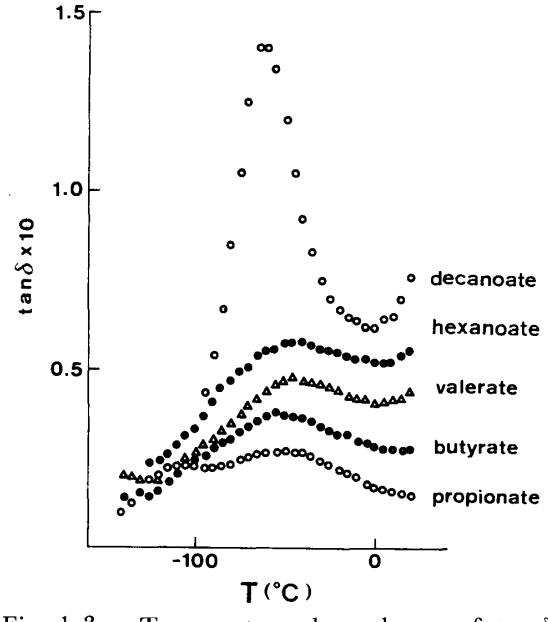

Fig. 1-3a. Temperature dependence of tan δ at 11 Hz for the acylates from propionate to decanoate.

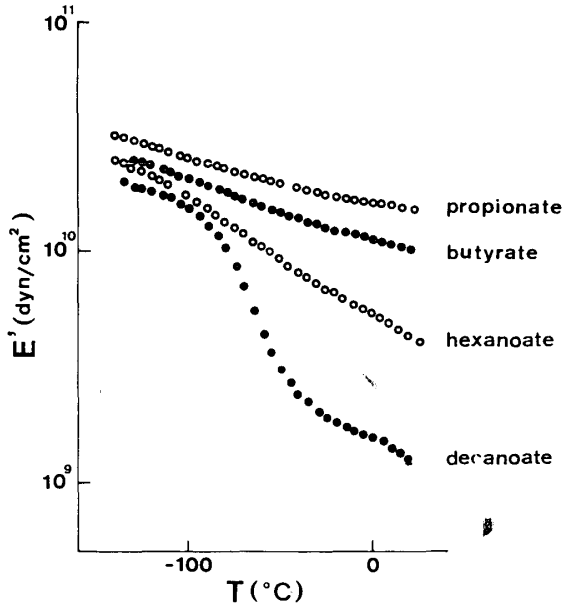

Fig. 1-3b. Temperature dependence of E' at 11 Hz for the acylates from propionate to decanoate.

the specific loss, the ratio of the energy dissipated to the energy stored per quarter cycle, while E'' corresponds to the absolute energy dissipated. The plots of tan δ and E' at 11 Hz against tamperature for the acylates in the temperature region of the β_m process are shown in Figures 1-3a and 1-3b, respectively. The β_m peak increases in height with increasing n. Corresponding to this, the relaxation magnitude increases with increasing n as shown in Figure 1-3b. In particular, E' value for decanoate falls from 1.5×10^{10} dyn/cm^2 to 1.8×10^{9} dyn/cm^2 as the temperature rises from -100°C to -20°C. The plots of logarithm of the frequency at tan δ maximum against the reciprocal of absolute temperature are shown in Figure 1-4. There is a linear relationship between them. The value of ΔE

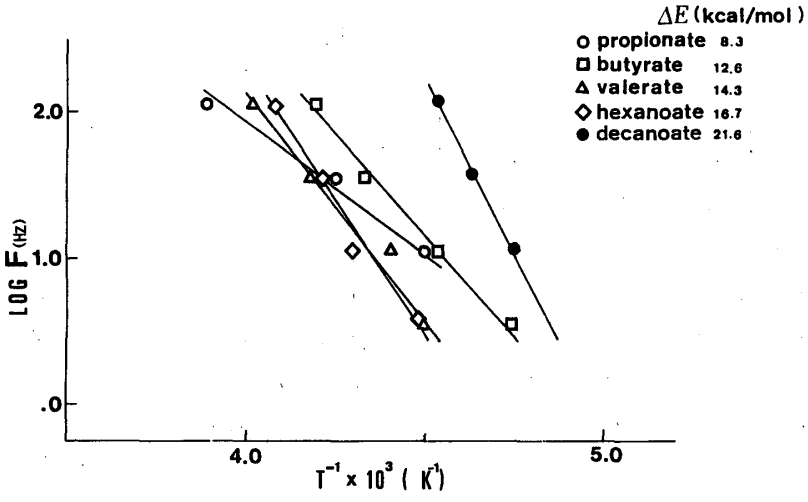

Fig. 1-4. Plots of logarithmic frequency (F) against the reciprocal of absolute temperature (T^{-1}) at tan δ maximum for the β_m process.

calculated from the slopes are also shown in the Figure. Obviously, the value increases with increasing n and that for (cellulose) decanoate seems to be somewhat large compared to that quoted usually for polymers in the glassy state. It should be emphasized that tan δ, ΔE and relaxation magnitude, increase with increasing the side chain length. From these findings, it is considered that the β_m process is due to the side chain motions of the acylates. A possible explanation for the motion of the side chain is as follows: when the side chain length is short as in (cellulose) propionate, the motion of molecular segment responsible for the β_m process may be restricted only to the hindered rotation or the twisting. In tihs case, ΔE for the motions is considered to be fairly small. On the other hand, when the side chain length is long enough as in the decanoate, a short range diffusional motion of the segments along the side shain, similar to a micro-Brownian motion along the main chain, may result in the β_m process, which requires large

ΔE. Therefore, it may be considered that the motion of the side chain responsible for the β_m process shifts from the hindered rotation or the twisting to the short range diffusional motion with increasing the side chain length.

1.4 The β'_m process

In Figure 1-3a, a shoulder at about -100°C occurs in tan δ versus temperature curve. This process labelled β'_m has appeared more distinctly in E'' versus temperature curves than in tan δ versus temperature curves as shown in Figure 1-5, in which E'' is plotted in arbitarary scale over the temperature range from -150°C to 20°C at 11 Hz.

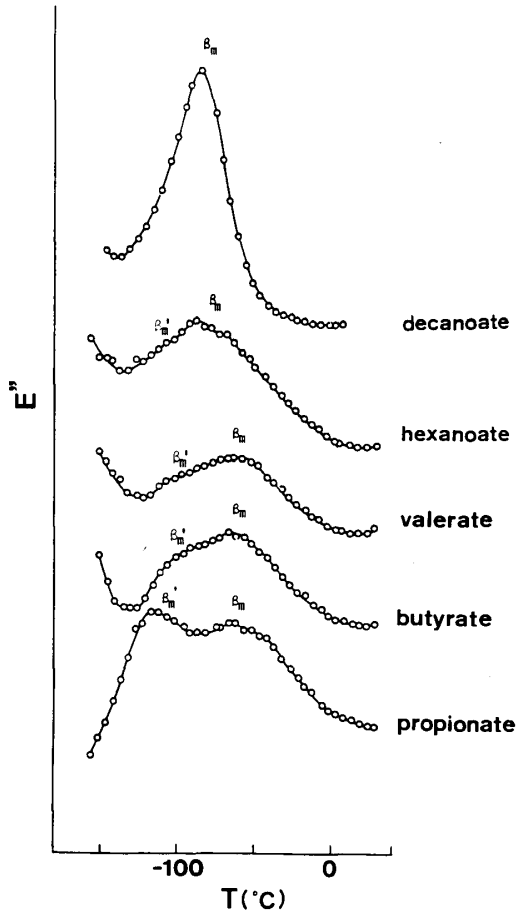

Fig. 1-5. Temperature dependence of loss modulus E'' at 11 Hz for the acylates from propionate to decanoate.

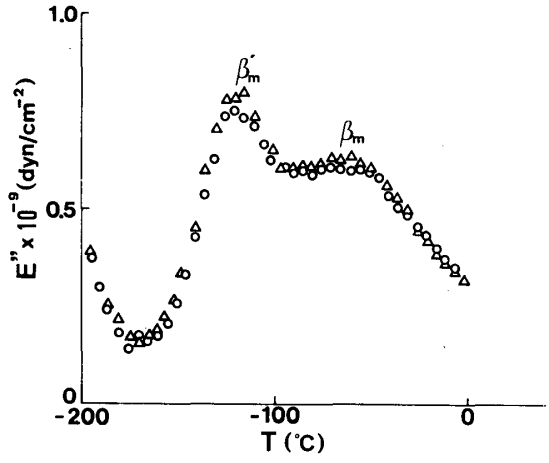

Fig. 1-6. Temperature dependence of loss modulus E'' at 11 Hz for cellulose propionate. △: immersed in water, ○: dried at 80°C for 40 hr in vacuo.

The β'_m peak, which is clearly observed for the propionate, becomes less distinct as n increased and at last merged completely into the β_m peak for the decanoate. In order to assign the β'_m process, the effect of water on the process for (cellulose) propionate was investigated and the results are shown in Figure 1-6.

As is evident from the figure, it can be seen that the β'_m process is independent of water absorbed. In this connection, it was found that the β_m process was also independent of water. From this fact, the cause of β'_m process should be attributed to the molecular motion of the acylates themselves. It can be considered that there is a remarkable difference in the degree of freedom of the motion of the side chains introduced at C-6 and C-2 or C-3 positions of a glucopyranose ring. Therefore, it is plausible that the side chains attached to the different positions cause substantially different relaxation mechanisms with each other. If the difference in the relaxation time among these side chain motions exists, then the resulting relaxation process ought to be different. Therefore, the β'_m process as well as β_m process may be due to the motion of the side chain.

1.5 The γ_m process

Figure 1-7 shows the variation of E'' with temperature for the acylates from

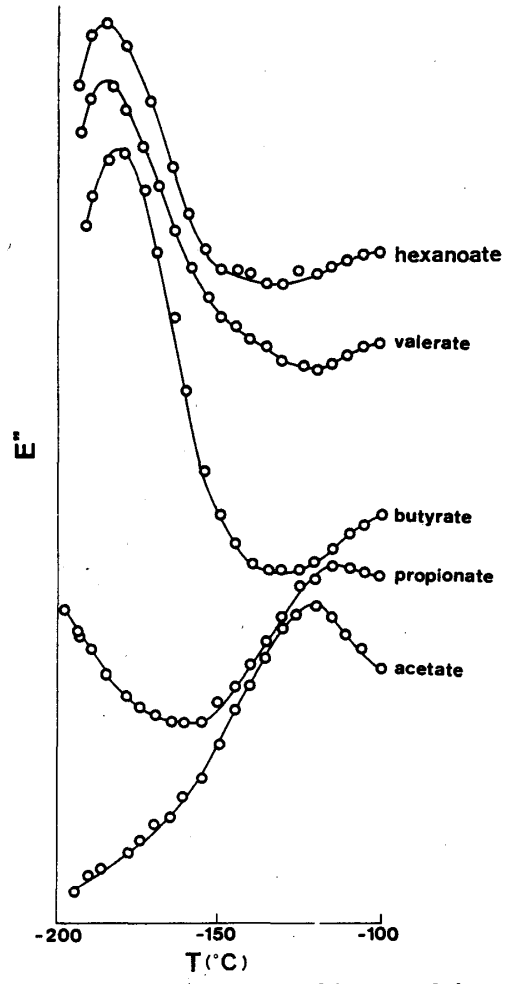

Fig. 1-7. Temperature dependence of loss modulus E'' at 11 Hz for the acylates from acetate to hexanoate.

acetate to hexanoate in the temperature range from −190°C to −100°C at 11 Hz. The relaxation process labelled γ_m is detected for the higher homologues above the butyrate at around −180°C. However, the process is not recognized for both the acetate and the propionate in the temperature range examined. By using the mechanical experiments, many investigators have reported that a relaxation process occurs in the temperature range from −100°C to −200°C at low frequencies for polymers involving at least three methylene groups (-CH_2-) in a row. Te ΔE for the γ_m process is calculated to be about 6.3 kcal/mol which is comparable to the values obtained for the polymers mentioned above. From these facts, the γ_m process can be ascribed to the motions initiated by -CH_2-CH_2-CH_2- parts of the side chain. It is of interest to note that E'' for the propionate increased with decreasing temperature in the range from −150°C to −190°C. For the propionate, the γ_m process can occur no longer because of the absence of -CH_2-CH_2-CH_2- portion in the side chain. However, in this case, the motion due to -CH_2-CH_2- part may exist. Supposing that the γ'_m process results from the motion of -CH_2-CH_2- parts in the side chain, then it may occur in a lower temperature region compared to that for the γ_m process, since the relaxation time for the motions of -CH_2-CH_2- segments is considered to be shorter than that for the -CH_2-CH_2CH_2- motions. Such being the case, the γ'_m process will not be observed for the acetate which lacks -CH_2-CH_2- parts. In fact, no relaxation process similar to the γ'_m process could be observed for the acetate in the corresponding temperature range. Accordingly, it can be considered that the γ'_m process is due to the motion initiated by -CH_2-CH_2- parts of the side chain.

2. Dielectric relaxation processes of cellulose acylates

One of the useful procedures for assigning the molecular relaxation processes of polymers is through altering chemical constituents systematically. In line with this, many types of side chains were introduced systematically in the synthetic polymers such as polymethacrylates or polyacrylates, and their relaxation mechanisms were investigated[29,30]. Poly-*n*-alkyl methacrylates, in particular, have been studied extensively by using mechanical or dielectric measurements. In this case, however, the glass transition (primary process) overlaps the secondary transition (secondary process) which is due mainly to the side chain motion, for a homologue with the side chain length longer than that for poly-*n*-butylmethacrylate[31]. This overlapping seems to arise from the similarity in both flexibility and motional unit of the main and side chains. As shown in Chapter 1, however, the primary (α_m) and secondary (β_m, β'_m) processes for the acylates with a long side chain appeared separately though *n*-alkyl groups are introduced in the side chain as in poly *n*-alkyl methacrylates. This suggests that the flexibility of the

main chain which consists of bulky glucopyranose units, is more restricted than that of the side chain.

From the above consideration, the study on the relaxation processes for the acylates by introducing side chains longer than those in Chapter 1 is worth to carry out. This chapter describes dielectric relaxation processes of thirteen kinds of the acylates from the acetate to stearate[32], in detail, in relation to the mechanical processes examined in Chapter 1. The dielectric measurements were made for powdered samples pressed into uniform compact discs 5 cm in diameter and 0.7 mm in thickness. Using a transformer bridge, dielectric constant and dielectric loss were measured over the frequency range of 50 Hz to 1.0 MHz and the temperature range of −190°C to 200°C. The melting of the acylates was observed by using a thermomechanical analyzer (TMA), in which a column of the sample collapsed under a plunger which was driven by a constant load of 3 kg/cm^2, when heated at a uniform rate of 1°C/min. The TMA analysis is also employed in Chapters 3, 5, and 10.

2.1 Characterization of the samples

Table 2-1 shows the number of carbon introduced in the acyl side chain, n, the degree of substitution, DS, the avarage molecular weight, M_W, and the melting point, T_m, for a series of cellulose acylates from acetate to the stearate prepared. The M_W values are of the order of about 10^5. The values of DS determined by saponification method for the acylates up to $n=8$ exceed 2.8. However, determination of DS by using saponification method became inaccurate for the acylates above $n=9$. Therefore, instead of saponification method, DS of the samples above $n=9$ was estimated by IR spectrometry.

Table 2-1. Characteristics of the acylates used

The Acylates	n	DS	M_W	T_m (°C)
Acetate	2	2.83	—	278
Propionate	3	2.96	1.48×10^5	241
Butyrate	4	2.80	1.77×10^5	189
Valerate	5	2.79	2.15×10^5	128
Hexanoate	6	2.83	2.15×10^5	110
Enanthate	7	3.04	2.07×10^5	103
Octanoate	8	2.84	2.03×10^5	93
Pelargonate	9	—	3.54×10^5	87
Decanoate	10	—	2.32×10^5	102
Laurate	12	—	2.18×10^5	112
Myristate	14	—	2.87×10^5	108
Palmitate	16	—	3.98×10^5	113
Stearate	18	—	6.91×10^5	121

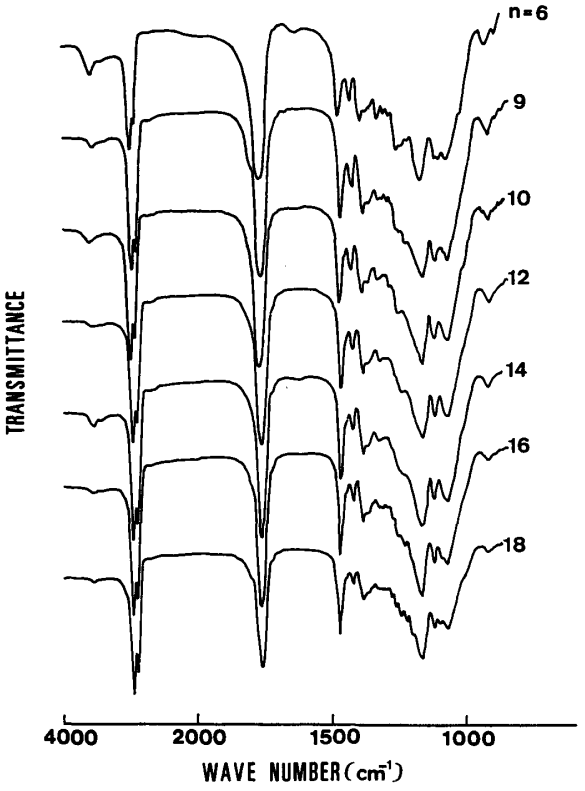

Fig. 2-1. Infrared spectra of the acylates. n: the number of carbons in the acyl side chain.

Figure 2-1 shows IR spectra for the valerate to the stearate. Absorption intensity of OH stretching band in the vicinity of 3,600 cm^{-1} for the acylates above $n=9$ is smaller than that for the valerate whose DS value is 2.79. From these results, all the acylates prepared are thought to be almost fully acylated.

In order to define the melting point T_m of the sample, comparisons of the temperature were made as determined by the following two types of measurements. One way is measuring the temperature, T_{m1}, at which the samples when heated at a constant rate became quickly transparent under microscopic observation. The second process is measuring the temperature T_{m2} at which the plunger in TMA reached the bottom of the glass capillary, indicating transition from solid state to liquid state. Both temperatures thus obtained coincided closely. Therefore, in this report, both T_{m1} and T_{m2} can be used as T_m. In the table, T_{m1} is shown as T_m of the sample.

Figure 2-2 shows the variation of $T_m(T_{m1}, T_{m2})$ with n for the acylates. The values of T_m decrease abruptly with increasing n up to 5, i.e. they fall from 300°C to 128°C as n increased from 2 to 5. However, even if additional acyl methylene units were added in the formation of the higher homologues ($n=6$ or higher), T_m remains almost unchanged. In the same figure, the results of the acylates prepared

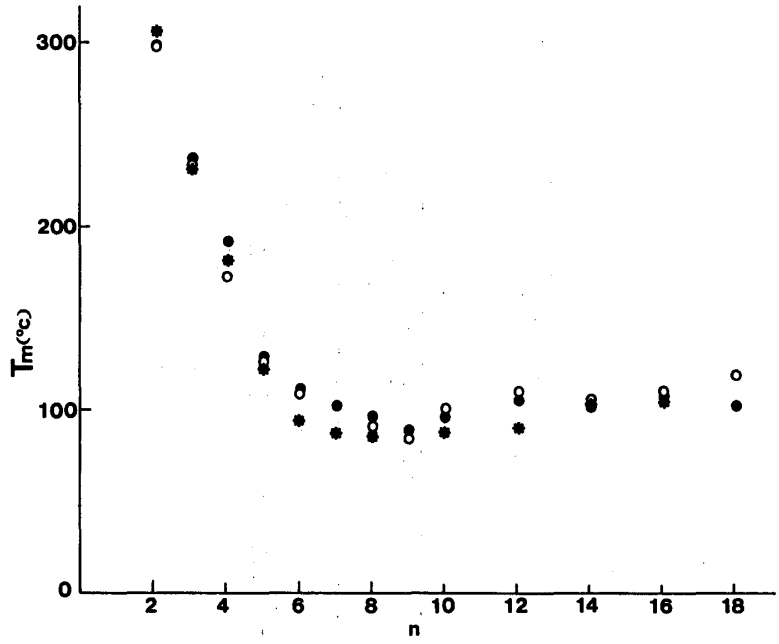

Fig. 2-2. Dependence of the melting point (T_m) on the number of carbons (n) in the acyl side chain: (○) micrographic observation; (●) TMA; (*) after Malm et al.

by Malm et al.[33] by using acid chloride-pyridine esterification are also shown. Obviously, they are in fair agreement with those of auther's samples.

2.2 Contour diagrams of dielectric relaxatin

For the acylates characterized above, dielectric relaxation experiments were carried out. Figure 2-3 and 2-4 give variation of the dielectric loss ε'' for the valerate and the palmitate, respectively, as a function of the temperature and frequency, i.e. contour diagrams. In these Figures, three types of relaxation processes

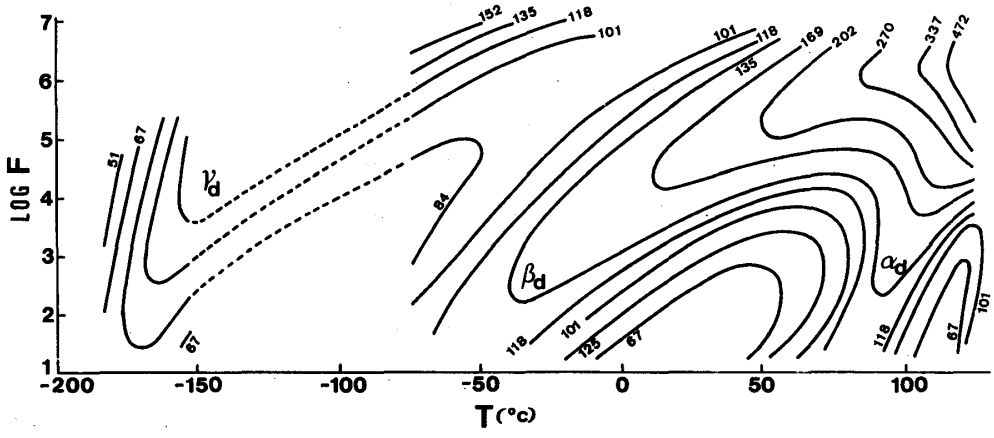

Fig. 2-3. Contour diagrams of the dielectric loss ε'' for the valerate as a function of logarithmic frequency (F) and tamperature (T). ε'' value given in unit 10^{-4}.

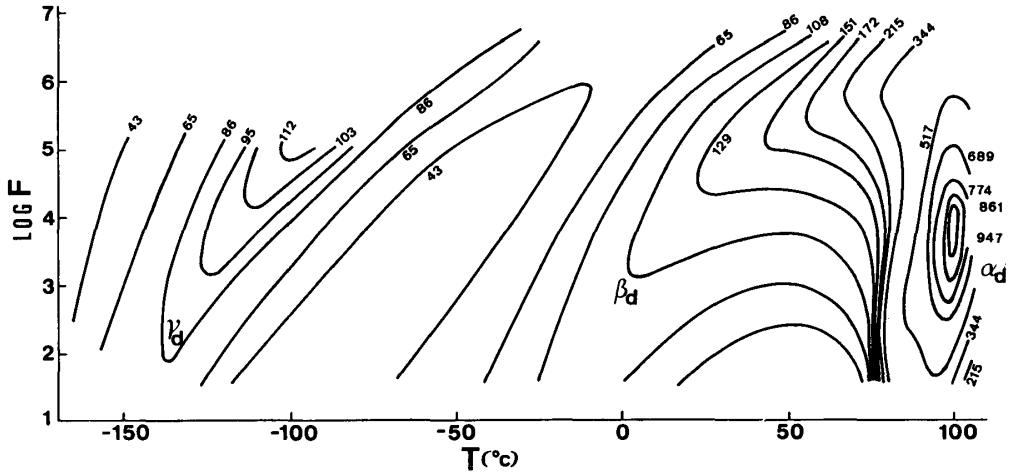

Fig. 2-4. Contour diagrams of the dielectric loss ε'' for the palmitate as a function of logarithmic frequency (F) and temperature (T). ε'' value given in unit 10^{-4}.

can be recognized, and they are labelled α_d, β_d, and γ_d in order of decreasing temperature or in order of increasing frequency at which they were detected. Also, for the butylate to the stearate three relaxation processes (α_d, β_d, and γ_d) similar to those for the valerate or the palmitate are obtained. However, the α_d process for the acetate and the γ_d for both acetate and propionate are not observed. On the contrary, a relaxation process, labelled γ'_d, is detected for the propionate. It should be emphasized that the α_d and the β_d processes are observed separately in the contour diagrams even for the acylates having a side chain with length long enough as in the stearate; this is quite different from the case of poly-*n*-alkyl methacrylate[31]. In the following, the molecular mechanism for these α_d to γ_d processes will be discussed, in sequence, in relation to the mechanical processes (α_m, β_m, γ_m, and γ_m') described in Chapter 1.

2.3 The α_d process

The α_d process is observed in the higher temperature and in the lower frequency region prior to the melting of the sample (Fig. 2-3 and 2-4). Regarding the α_d process, the value of apparent activation energy ΔE for n from 3 to 6 decreases with increasing n, i.e. 160, 67, 58, and 50 kcal/mol, respectively, but for n above 6, it remains at a constant value of about 50 kcal/mol. In connection with the α_d process, Mikhailov et al.[24] found a process, having a ΔE of 70 kcal/mol for the acetate at a frequency of 10 kHz at 220°C by using dielectric measurements. Judging from both the temperature frequency location and the ΔE value, this process can be classified as the α_d process. Therefore, the α_d process is thought to appear in all the acylates examined. Corresponding to this, the location of the α_d process for each acylate is comparable to that of the α_m process described above.

From these findings, the α_d process as well as the α_m process are considered due to the micro-Brownian motion of the main chain. Thus, the α_d process is related to the glass-rubber transition of the acylates. Accordingly, the temperature location of ε'' maximum at a low frequency for the α_d process can be regarded as a rough measure of the glass transition point T_g of the sample. Corresponding to the result for the α_m absorption at a low frequency in Chapter 1 (Section 2), the T_g thus defined shifts markedly to lower temperature with increasing n up to 6, because these two reflect the same mechanism. However, the T_g seems to level off when n reached 6. These trends recognized for T_g are parallel to those for the melting points of the sample (Fig. 2-2). On the other hand, it has been reported that the T_g for poly-*n*-alkyl methacrylates decreases continuously with increasing n, reaching −65°C for poly-*n*-dodecyl methacrylate[27]. This difference between cellulose acylate and poly-*n*-alkyl methacrylate, both involving long *n*-alkyl groups in the side chain, may be attributed to the different structure of the main chain; the former is bulkier than the latter.

2.4 The β_d process

As the acetyl content in cellulose increases, the relaxation process due to the orientation of methylol groups becomes less distinct, but instead, the β_d process appears[35]. Many investigators have reported on the β_d process in acetate, and they attributed this process mainly to the hindered rotation of the acetyl group[18,20,36–38]. As stated in Section 2.2, however, it should be noted that the β_d process is recognized not ony for the acetate but also for all the other acylates examined. This fact means that the β_d process reflects motions within the acyl groups. In order to assign the β_d process, plots of logarithmic frequency at ε'' maximum

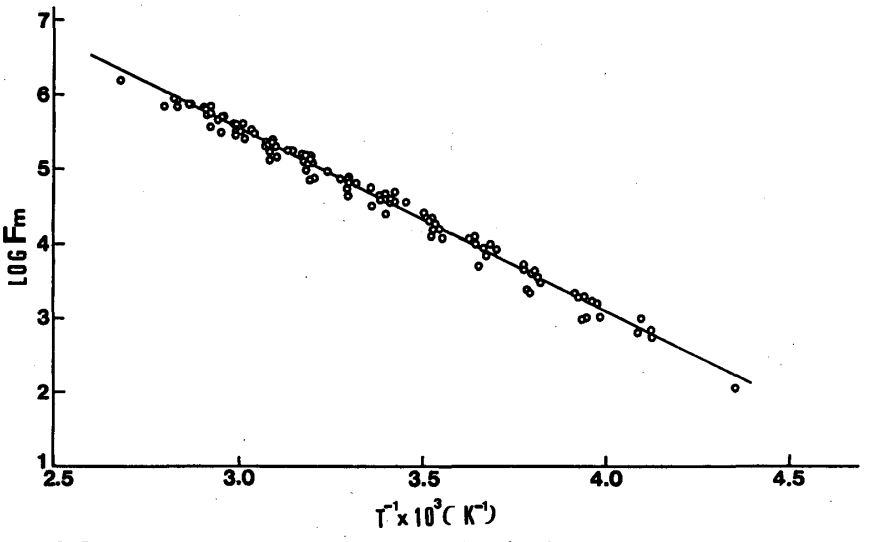

Fig. 2-5. Plots of logarithmic frequency (F_m) at ε'' maximum against reciprocal of the absolute temperature T^{-1} for the β_d process.

against the reciprocal of the absolute temperature, i.e. transition map, for all the acylates are shown in Figure 2-5. In the Figure, several plots which are discussed in a later section (2.5) are not included. It is to be noted that all the resulting plots are on one straight line. By means of least square method, this line is expressed by the equation,

$$\log F_m = -2459 T^{-1} + 12.91, \qquad (1)$$

with a correlation coefficient of 0.994. The ΔE value calculated is 11.3 kcal/mol, which is comparable to that reported for the β_d of the acetate[36-38]. The finding that the β_d process for all the acylates gives the same ΔE and relaxation time means that this process results from a dielectrically active common unit in the acyl side chain. Such a unit is the oxycarbonyl groups attached to the glucopyranose ring. Thus, it is concluded that the β_d process can be regarded as due to the orientational polarization of the oxycarbonyl group in the side chain. Furthermore, dielectric examination of 2, 3-di-*O*-acetyl-6-*O*-trityl cellulose reveals that the process arises from the motion of oxycarbonyl groups which are introduced not only at C-6 position but also at C-2 and C-3 positions of a glucopyranose ring[39].

Concerning the acetate, however, my conclusion does not necessarily contradict the assignments proposed by other investigators. Since the acetyl side chain is substantially small in molecular size, the motion of oxycarbonyl groups in the acetyl side chain cannot be distinguished from that of the acetyl side chain itself. In fact, for the acetate the β_m process due to the side chain motion (see 1.3) was detected in the temperature and frequeny ranges comparable to those for the β_d process[22]. Hence, the β_d process can be approximately attributed to the motion of the side chain when it is small enough as in the acetate.

Table 2-2 shows ΔE, activatation entropy ΔS, and activation freee nergy ΔF for both the β_d process of cellulose acylate and the process due to the motion of methylol group of cellulose I and II. Apparently, the value of ΔE for the two types of molecular relaxation is the same. The ΔS value for the β_d relaxation is small as compared to that for the relaxation of the $-CH_2OH$ group. This indicates that the motion of oxycarbonyl group is somewhat restricted as compared to that of the methylol group; this corresponds to the fact that the

Table 2-2. ΔE, ΔS and ΔF for cellulose and the acylates

Samples		Relaxation	ΔE (kcal/mole)	ΔS (eu)	ΔF (kcal/mole)
Cellulose*	I	CH_2OH group	10.1	9.3-10.2	7.5- 8.0
	II		10.6	9.8-10.4	7.6- 8.2
The Acylates		β_d (n: 2-18)	11.3	0.7- 3.6	9.7-10.4

* Cellulose I=Whatman cellulose CF-11; Cellulose II, prepared by saponification of the acetate.

former appears in the higher temperature and lower frequency regions than the latter.

2.5 Micro-Brownian motion of the side chain

In order to obtain further information on the β_d process, the transition map for the acylates above $n=12$ is shown in Figure 2-6, in which several plots ommited in the Figure 2-5 are also included. Plots for each sample in the lower temperatures which were not on the line expressed by eq. (1) described above, instead, are lines with greater slope than the line one (1). In the Figure, the temperatures at the intersecting points, T_0, between the line (1) and the other lines are denoted by arrows. The T_0 apparently shifts to a higher temperature region (−15, 12, 27, and 34°C) with increasing n (12, 14, 16, and 18). This phenomenon is analogous to the dependence of the glass transition temperature on the molecular weight. The ΔE for the respective acylates in the temperature region below T_0 becomes somewhat larger than that above T_0, ranging from 18.6 to 20.4 kcal/mol. This suggests that the orientation motion of the oxycarbonyl group becomes restricted in the temperature range below T_0. Although the β_m process as well as β'_m are not identical in relaxation machanism with the β_d process, the results of the corresponding dynamic mechanical measurements in Chapter 1 are available, in order to understand this phenomenon. In the case of the cellulose decanoate ($n=10$), the region in which β_m occured was at the temperature of about −60°C and at frequency 11 Hz. This process was considered to reflect a micro-Brownian motion of the side chain. Therefore, the freezing temperature of the side chain for $n=10$ can be thought to be about −60°C. On the other hand, when the

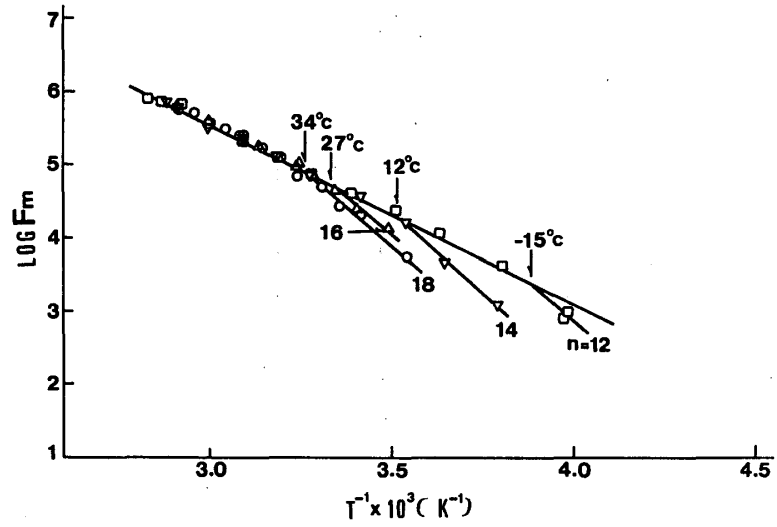

Fig. 2-6. Plots of logarithmic frequency (F_m) at ε'' maximum against reciprocal of the absolute temperature T^{-1} for the β_d process for the samples $n=12$ and above.

relationship between n and T_0 is extrapolated into the case of $n=10$, T_0 could be estimated to be -60°C. These findings indicate T_0 to be the freezing temperature of the micro-Brownian motion of the acyl side chain. Supposing that the side chain froze in the temperature region below T_0, then the orientation of the oxycarbonyl group which is a part of the side chain will be restricted. Hence, the ΔE value below T_0 becomes larger than that above T_0.

2.6 The γ_d and γ'_d processes

As was shown in Figures 2-3 and 2-4, the γ_d process is detected in the lowest temperature and the highest frequency region examined. The γ_d peak decreases gradually in height with an increase in n. However, this process is not observed for samples with $n=2$ or 3, corresponding to the results of the γ_m process for the samples (See Section 1.5). Figure 2-7 shows the transition map for γ_d above $n=4$. The resulting plot for each acylate is expressed by a straight line and the ΔE value ranges from 5 to 8 kcal/mol. For n less than 7, lines are similar in location, but for n greater than 8 they shift higher temperature with increasing n. The temperature frequency location and the ΔE value for the γ_d process are comparable to those for the γ_m process. Accordingly, it is considered that both γ_d and the γ_m processes are associated with the same molecular relaxation. In Chapter 1 (Section 5), the γ_m process was ascribed to the motion initiated by three or more methylene groups in the side chain. However, since methylene groups are non-polar, the motion of the dipolar oxycarbonyl group adjacent to the methylene groups has to be included in the γ_d process. From this, both the γ_d and γ_m processes are thought to be due to the motion of three or more methylene groups including the motion of the oxycarbonyl group in the side chain. In this connection, the relaxation process

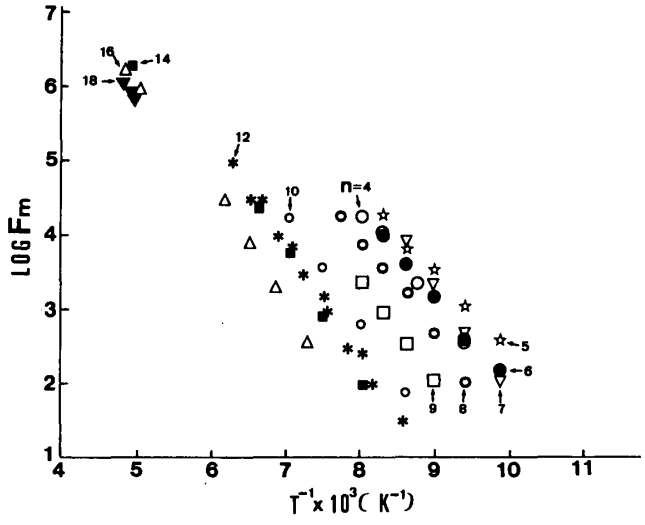

Fig. 2-7. Plots of logarithmic frequency (F_m) at ε'' maximum against reciprocal of the absolute temperature T^{-1} for the γ_d process.

which involves motions of dipolar component in addition to those of the three or more methylene groups has been already reported for many synthetic polymers including poly-*n*-alkyl acrylate, poly vinyl esters, polyamids, and oxide polymers[20]. However, auther's systematic experiments indicate that the γ_d process should be regarded as due, at most, to the motion of $-CH_2-CH_2-CH_2-$ parts associated with the motion of the neighbouring oxycabonyl group, since the magnitude of the γ_d absorption for $n=4$ is the largest of all the acylates examined, and it decreases continuously with increasing n. In addition to the γ_d process, I have to state the existence of the γ'_d process, instead of γ_d, in the propionate. However, the γ'_d process is detected only as a rise in ε'' with increasing frequencies in the lowest temperature examined. This process may be attributed to the oxycarbonyl group of the propionate in a similar manner as that for the γ'_m process.

PART II Acylated Cellulose Prepared in FD/DMSO solvent

3. Mechanical relaxation processes of (celluloe oligo-oxymethylene ether) acylates

Johnson et al.[7] reported that cellulose is soluble in dimethyl sulfoxide (DMSO) in the presence of paraformaldehyde (PF). The mechanism by which cellulose dissolves in the PF/DMSO mixture was shown to involve the formation of cellulose oligo-oxymethylene ether[40]. Although, C-6 position of glucopyranose ring seems to be preferred for substitution, there is nmr evidence that the oxymethylene groups are also located at C-2 and C-3 positions. The homogeneous chemical modification of cellulose in the PF/DMSO medium could open the field to the development of new cellulose derivatives.

The acylation of cellulose in this solvent results in novel cellulose polymers (cellulose oligo-oxymethylene ether) acylates, COAs. Their physical properties are expected to be quite different from the corresponding conventional cellulose acylates described in PART I. In fact, the thermal softening properties of (cellulose oligo-oxymethylene ether) acetate[17] were found to be conspicuously different from cellulose triacetate; the apparent melting temperature of the former is about 140°C lower than the published melting point of cellulose acetate. In this connection, the thermal softening of silyl cellulose[16] was found to be considerably reduced by the indroduction of oligo-oxymethylene in the side chain.

This chapter surveys viscoelastic properties of a series of COAs from the acetate to the valerate[41]. The method for the preparation of cellulose solution used in this study was essentially similar to that reported by Johnson et al.[7]. Dried cellulose powder (2 g) and paraformaldehyde, PF (4 g) were well dispersed in DMSO (50 ml) at room temperature. The mixture was then heated with vigorous stirring to

120°C over a period of about 20 min in a 100 ml Erlenmyer flask equipped with a condencer (a ground-glass jointed tube). After being held at this temperature for 3 hr, the cellulose solution so obtained was cooled to room temperature. To the cooled cellulose solution, triethylamine, TEA (6 mol/mol glucose anhydride unit of cellulose) and one of a series of aliphatic anhydrides from acetic anhydride to valeric anhydride (6 mol/mol glucose) were added dropwise. After the addition, the reaction mixture was allowed to stand at room temperature for 5 hr. The reaction mixture was then poured into precipitants. Samples obtained are peracylated. The similar procedure was used for the preparation of other acylates in PART II. In some cases, however, the dissolution condition (time and temperature) of cellulose different to the above is employed.

3.1 Thermal softening properties

When the thermoplastic samples were heated under a constant load at a uniform rate, the deformation of the sample gradually increased. From the resulting thermal deformation diagram, information on physical transitions and melting can be derived. Figure 3-1 shows diagrams of thermal deformation ($\boldsymbol{D}$) vs. temperature (T) for a series of COAs from acetate through valerate. In the diagrams the deformateon $\boldsymbol{D}$ is normalized, i.e., $\boldsymbol{D}$ is zero at room temperature and unity at the tempereture T_f at which the plunger in TMA (See Chapter 2) reached the bottom of the glass capillary, indicating completion of liquid flow of the sample. The thermodiagrams exhibit two well-difined transition regions. The first region is

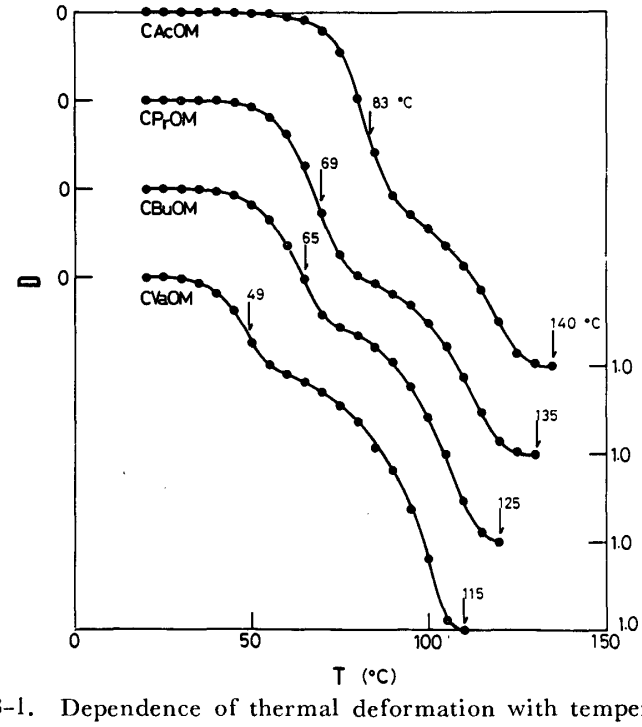

Fig. 3-1. Dependence of thermal deformation with temperature.

considered to be due to the glass transition and thus the rapidly changing deformation can be ascribed to the short-range diffusional motion of the segments along the polymer chain. In this region, the temperature T_s is defined as a temperature corresponding to the dD/dT maximum. The temperature T_s for the four kinds of COAs were 83, 65, 69, and 49°C in order of increasing number of carbons (n) in introduced acyl groups. Apparently T_s shifts to a lower temperature as n increases. T_s is considered as a rough measure of the glass transition point T_g.

3.2 Comparison of melting temperature between COAs and cellulose acylates

The second region in Fig. 3-1 indicates an apparent state of liquid flow of the polymer chain. Judging from the X-ray diagrams for COAs, they are completely amorphous. In general, amorphous polymers do not have a well-defined melting point T_m. Therefore, in this chapter, instead of T_m, the temperature T_f is used as a measure of the melting temperature of samples.

In Figure 3-2, the variation of T_f with n for both cellulose acylates described in Chapter 2 and COAs is shown. With increasing n less than 5, the value of T_f decreased slightly for COAs, but markedly for cellulose acylates. However, even if additional acyl methylene units were added in the formation of the higher homologs (n=6 and higher), T_f remained fairly constant. It is of interest to note that the value of T_f for (cellulose oligo-oxymethylene ether) acetates (CAcOM), differs substantially from that for cellulose acetates (CAc): ca 140°C lower for the former than for the latter. The reason for a considerable lowering of T_f for

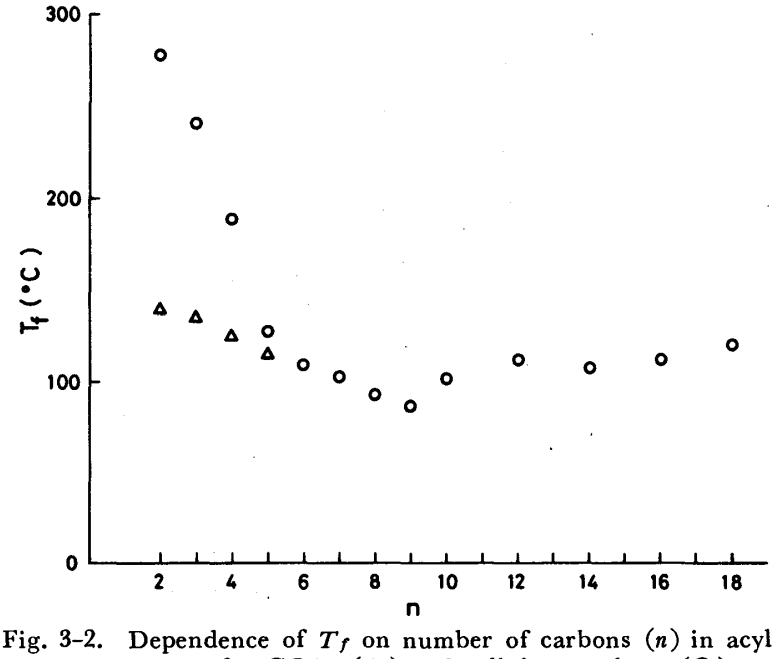

Fig. 3-2. Dependence of T_f on number of carbons (n) in acyl groups for COAs (△) and cellulose acylates (○).

COAs compared to that for cellulose acylates can be ascribed to the weakening of interchain cohesive force. In this connection, it can be noted that the value of T_f for CAcOM is similar to that of cellulose valerate, CVa. This result may be related to the fact that the contour length of the side chain for CAcOM has a magnitude of about 0.9 nm, corresponding to that for CVa.

3.3 Tensile properties

Figure 3-3 shows the stress-strain diagrams for COAs in tension measured at 20°C and 65%RH. These diagrams are similar in shape and have a yield point. In general, a yield point is observed in the stress-strain diagrams obtained at a

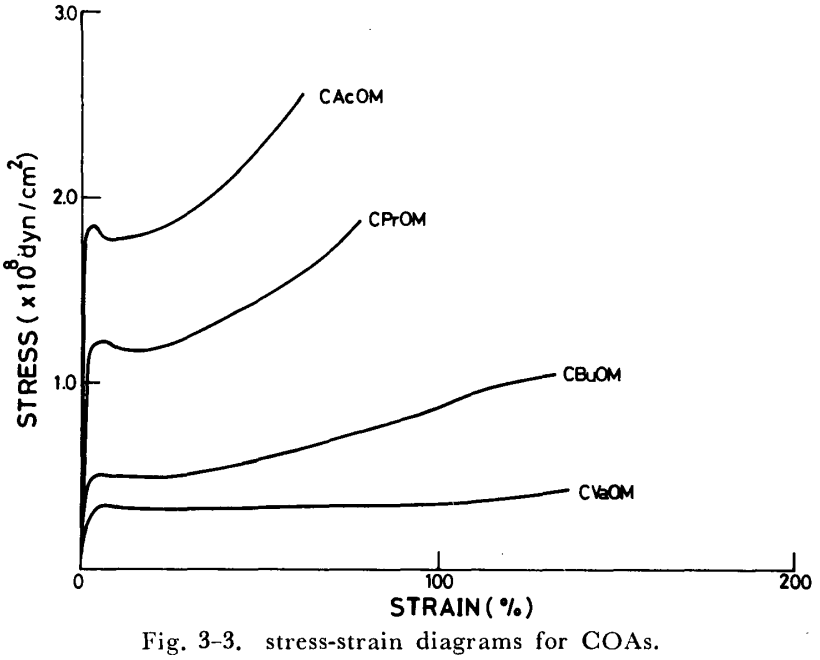

Fig. 3-3. stress-strain diagrams for COAs.

temperature in the neighborhood of T_g of the sample. However, it is evident that T_g of COAs is found to be somewhat above room temperature. On the other hand, it has been reported that polymeric materials having a marked subtransition below T_g usually exhibit a yield point in their stress-strain diagrams when they are obtained at around the subtransition temperature[42]. Therefore, it is suggested that for COAs a subtransition may occur at around room temperature. This point will be confirmed and discussed later by using dynamic modulus data. In Figure 3-4, the relationship between n and tensile strength σ, Young modulus E, or maximum elongation ε obtained from the stress-strain diagrams, is shown. It can be seen that by increasing n, values of σ and E decrease while the values of n increase. In particular, the values of σ, E, and ε for CAcOM were 2.58×10^8 dyn/cm^2, 1.08×10^{10} dyn/cm^2, and 0.59, respectively, which were within the range of corresponding values reported for various high-density polyethylenes.

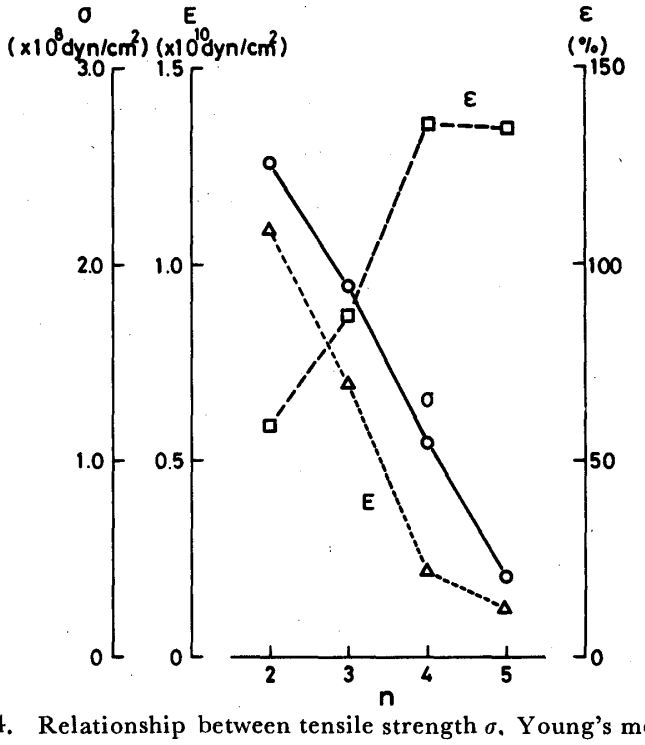

Fig. 3-4. Relationship between tensile strength σ, Young's modulus E, or maximum elongation ε and number of carbons (n) in acyl groups in COAs.

3.4 A survey of the relaxation processes

One of the most convenient ways of understanding the viscoelastic properties of polymers is through a modulus-temperature curve at a fixed frequency. Figure 3-5 shows the variation of dynamic modulus E' with temperature for COAs at 35 Hz. At about -190°C, E' values are from 7.5×10^{10} to 6.3×10^{10} dyn/cm^2, typical values for the polymer in the glassy state. If comparisons are made at the same temperature, the E' values decrease with increasing n in the temperature region examined. On the other hand, in higher temperature range a remarkable drop in E' is observed. E' is a value of the order of 10^7 dyn/cm^2 or less than 10^7 dyn/cm^2 at about 100°C. Especially, the change in value of E' for CAcOM fell from 10^{10} to 10^7 dyn/cm^2 as the temperature rose from 50°C to 120°C. This can be explained in terms of the glass-rubber transition. Furthermore, the glass transition region shifts to a lower temperature with increasing n. This phenomenon is interpreted as follows: the increase in the size of non-active n-alkyl groups causes decreased interaction of dipole ester group, to facilitate the chain backbone motion. The effect, known as internal plasticization, is similar to that produced by the addition of plasticizer, known as external plasticization. In the temperature range slightly below the glass transition, a considerable change in E', a subtransition, can be detected. For example, this transition for (cellulose oligo-oxymethylene ether)

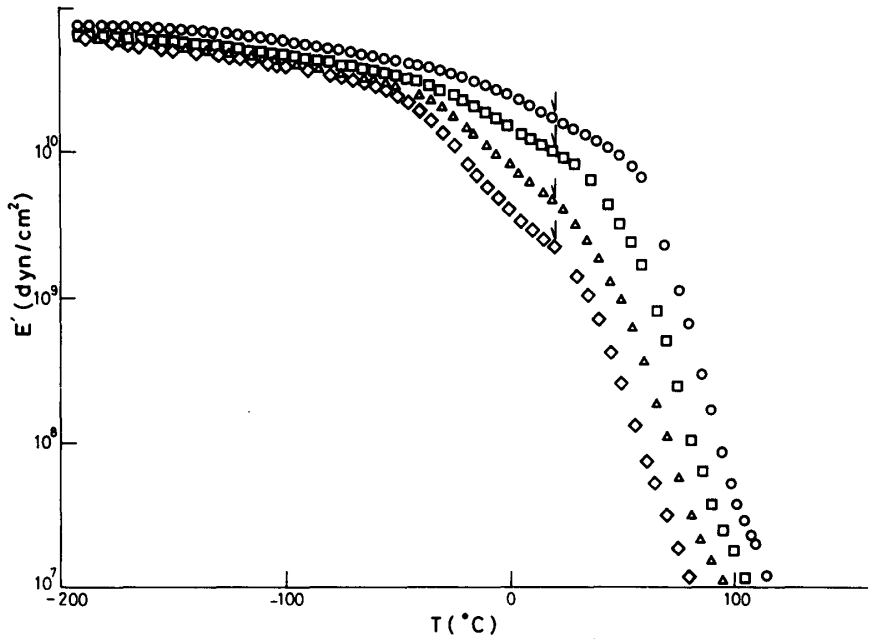

Fig. 3-5. Temperature dependence of dynamic modulus E' for COAs: CAcOM (○); CPrOM (□); CBuOM (△); CVaOM (◇).

valerate (CVaOM), located in the temperature range from −50°C to 30°C and the relaxation magnitude extends from 2.5×10^{10} to 1.5×10^{6} dyn/cm². In this connection, the stress-strain diagrams discussed above (Fig. 3-3) were obtained at the temperature denoted by arrows. The temperatures adopted for the static tensile tests for CAcOM and CVaOM correspond to those in the intermediate and terminal positions in the subtransition region, respectively. In the stress-strain diagrams, the former, CAcOM, gives a stress-strain diagram with a typical feature for hard and tough type of polymers and the latter, CVaOM, a typical feature for elastomeric materials.

3.5 The α and δ processes

The variations of E', loss modulus E'', and loss tangent tan δ with temperature for CAcOM at 35 Hz is shown in Figure 3-6. With respect to E'', three relaxation processes were detected within the experimental frequency and temperature range, being labelled α, β, and γ in order of decreasing temperature at which they were detected. The α process appeared as a high-temperature shoulder to the β process. Both the β and γ processes were broad in shape and overlapped. The same tendency was obtained by the corresponding measurements at 3.5, 11, or 110 Hz. The tan δ plot also revealed these three processes, but, in this case, both the β and γ processes appeared as a shoulder, while the α process exhibited a marked peak. For the α process, the drop in E' was from 10^{10} to 10^{7} dyn/cm² and the value of tan δ exceeded unity. From this evidence, the α process in CAcOM was

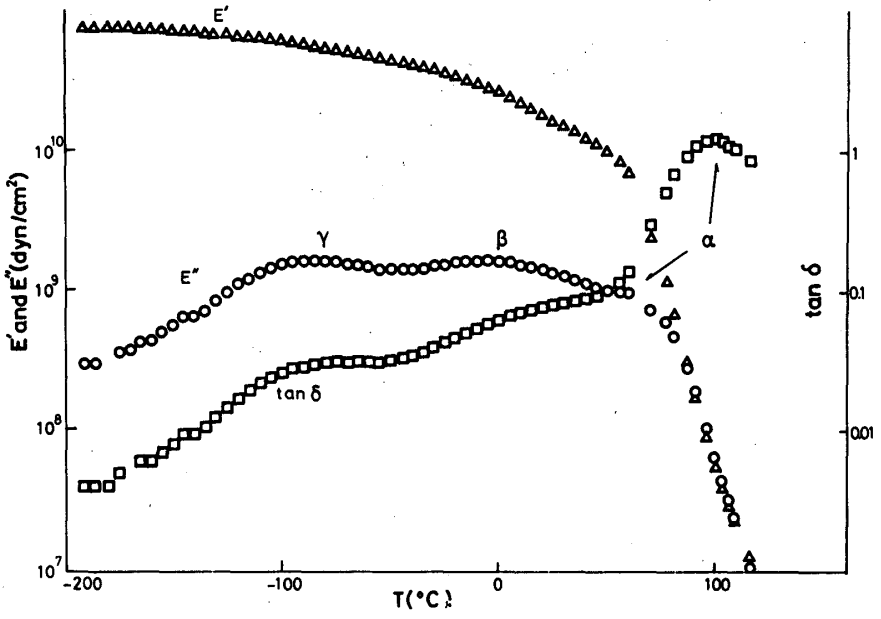

Fig. 3-6. Temperature dependence of dynamic modulus E', loss modulus E'', and loss tangent $\tan\delta$ for (cellulose oligo-oxymethylene ether) acetate at 35 Hz.

attributed to the segmental motion within the main chain, namely a micro-Brownian motion. In addition, for (cellulose oligo-oxymethylene ether) propionate (CPrOM), butylate (CBuOM), and CVaOM, three processes (α, β, and γ) similar to those for CAcOM were also observed at the temperature range between −200°C and 120°C at

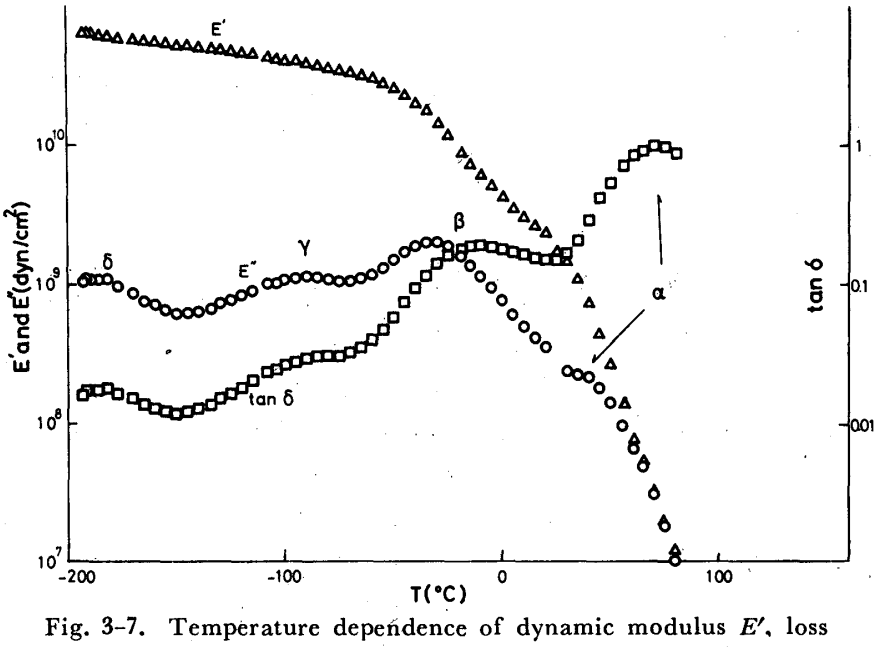

Fig. 3-7. Temperature dependence of dynamic modulus E', loss modulus E'', and loss tangent $\tan\delta$ for (cellulose oligo-oxymethylene ether) valerate at 35 Hz.

35 Hz. In the same manner, the α processes can be assigned to a micro-Brownian motion of each main chain. Figure 3-7 shows the relationship between E', E'', tan δ and temperature for CVaOM at 35 Hz. With regard to E'', it seems that the α process is too small in magnitude to be detected. This fact is thought to arise from an unexpected drop in E' or complex modulus in the subtransition prior to the glass transition. However, the value of tan δ maximum for the α process was very large, slightly exeeding unity. In the temperature range below -150°C, an additional process occured, labelled δ. This δ process was also observed for CBuOM at a similar temperature and frequency ranges. However, it should be emphasized that such δ peak was not detected with CAcOM and CPrOM. For all polymers in which at least three methylene ($-CH_2-$) groups in a row are involved, a relaxation occurs at temperatures between -100°C and -200°C at frequency of the order about 10 Hz. Polymers showing the relaxation in this temperature and frequency range include polyethylene, most nylons[43], poly alkyl acrylate[44], and other polymers with hydrocarbon side chains with length equal to or longer than a normal propyl group. Thus, the δ process observed for CBuOM and CVaOM is regarded as due largely to motions initiated by $-CH_2-CH_2-CH_2-$ parts of the side chain.

3.6 The β and γ processes

The plots of E'' with linear scale against temperature for a series of COAs in the temperature range from -150°C to 120°C at a frequency of 11 Hz is illustrated in Figure 3-8. The α loss peak which is clearly visible for CAcOM, became less distinct as n increased, and finally, for CVaOM, it merged completely in the high

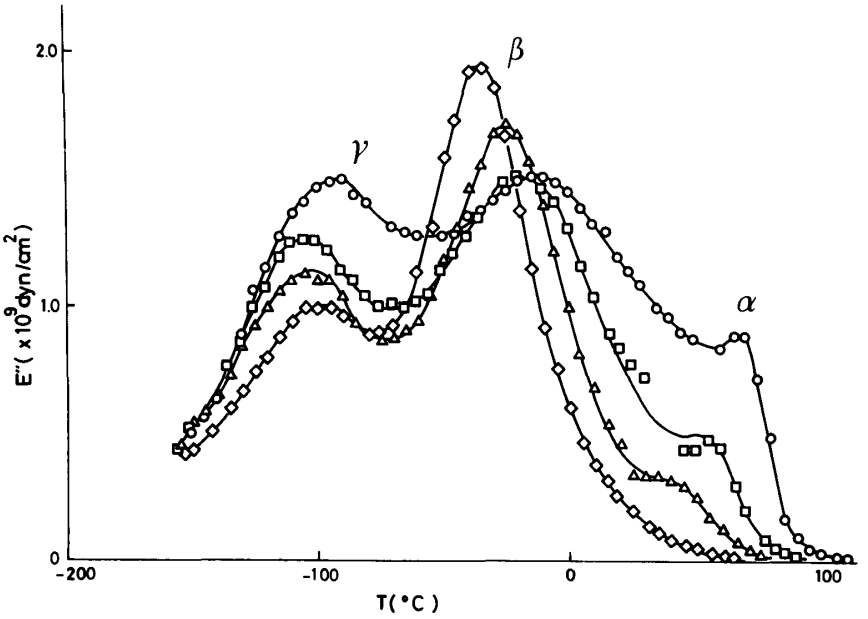

Fig. 3-8. Temperature dependence of loss modulus for COAs: CAcOM (○); CPrOM (□); CBuOM (△); CVaOM (◇).

temperature tail of the β peak. With increase in n, the β peak shifted apparently to lower temperatures, increasing in height and sharpening in shape. These phenomena concerning β processes seem intimately related to the fact that COAs have alkyl groups in the side chain. Thus, it is assumed that the β process is due to the relaxation of alkyl segments of COAs. If the alkyl segments in the side chain are responsible for the β relaxation, it is considered that the increase in the number of segments causes increased magnitude of E''. A possible explanation of the finding that the β region moves to lower temperature with an increase in n, is as follows: the increase in mobility of alkyl segments which results from further separation of the neighboring main chain with an increase in n. In this connection, similar peaks have been reported in the literature[45] for various kinds of synthetic polymers involving a long side chain such as poly (alkyl methacrylate). In such cases, however, occasionally the β peak cannot be determined precisely because of its overlapping with the α region.

Regarding the γ process, both the shape and the location appear to be relatively little affected by n. Furthermore, from the tan δ plots in the γ region, we see that the kinds of acyl groups does not essentially affect the γ process. Therefore, it can be regarded that the γ process reflects at least the same kind of intramolecular motion. On the other hand, as was shown in PART I, cellulose acylates do not exhibit the same kind of relaxation in the temperature and frequency ranges comparable to those for the γ relaxation in COAs. The difference in the molecular structure between the cellulose acylates and the COAs is essentially ascribed to whether or not they involve oxymethylene groups in the side chain. Hence, the γ process can be attributed to the motion of the oxymethylene portion in the side chain. However, this process will be assigned more directly by varing the length of oxymethylene chain in the next chapter.

3.7 Apparent activation energies for respective processes

The temperature-frequency locations-the relaxation map-of the three relaxation regions (α, β, γ) for COAs are summarized in Figure 3-9. The α plots were determined from tan δ-temperature curves, while the β and the γ plots were determined from the resolved E''-temperature curves. The reasons for this plotting are that the α peak is more distinct in tan δ curves than in E'' curves and that both the β and γ peaks are clearer in E'' curves than in tan δ curves. The β and γ processes, however, overlap. Therefore, an attempt was made to resolve the curves by supposing that each curve had a Gaussian form. As is evident from Figure 3-9, the plots for each process are approximately linear and similar in slope. The value of apparent activation energy ΔE for α process was calculated to be about 57.4 kcal/mol, which is of the order of principal dispersions. The

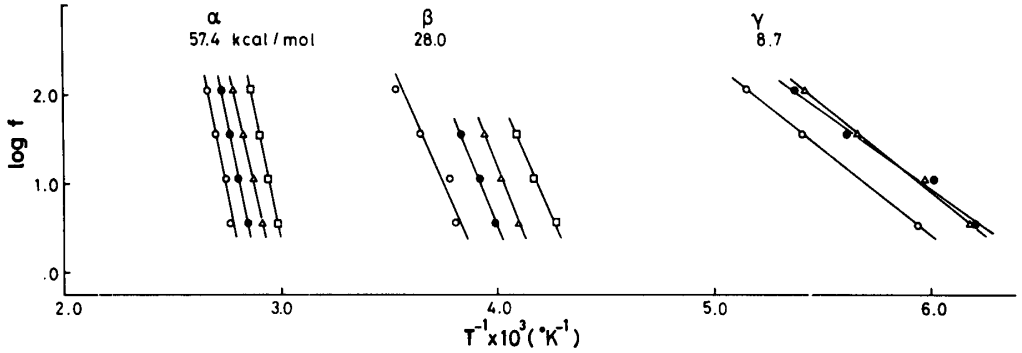

Fig. 3-9. Plots of $\log f$ vs. $1/T$ for loss maximum for COAs: CAcOM (○); CPrOM (●); CBuOM (△); CVaOM (◇).

value of ΔE for β was about 28 kcal/mol, an adequate value for the motion of the side chain. The ΔE value for γ process is about 8.7 kcal/mol, and the process is ascribed to the local mode motion involving oxymethylene groups.

4. Effect of oxymethylene and acyl side chain length on the relaxation processes in COAs

The COAs (cellulose oligo-oxymethylene ether) acylates, are different in chemical structure from the conventional series of cellulose acylates in that the oligo-oxymethylene groups are bonded between glucopyranose ring and the acyl side group. The length of the oligo-oxymethylene chain or the number of the oxymethylene unit introduced in respective COAs can be easily controlled through selection of dissolution condition of cellulose in paraformaldehyde/DMSO solvent system[46].

In Chapter 3, three relaxation processes (α, β, and γ) for all COAs and an additional process (δ) for the butylate and valerate were observed in the frequency and temperature ranges examined, and their molecular origins were discussed. Among these processes, the dominant α and β processes were shown to be largely affected by the kind of COAs, namely, the chain length of the linear acyl group introduced in the side chain. This indicates that the governing factor of the viscoelastic properties of COAs is its side chain length. However, the side chain of COAs is composed not only of acyl chain portion but also of oligo-oxymethylene chain portion. Therefore, it is important to clarify the effect of the length of oligo-oxymethylene chain on the viscoelastic properties of COAs.

This chapter describes dynamic mechanical properties of polymers in a series of COAs from acetate to decanoate in relation to the chain length of the oxymethylene portion as well as that of the acyl portion in the side chain[47]. All the samples employed here are almost amorphous in nature.

4.1 Degree of molecular substitution of oxymethylene groups

The acetyl contents (AC%) of cellulose acetate with *DS* value of 3.0 is known to be 62.5%. However, the AC% of (Cellulose oligo-oxymethylene ether) acetate, CAcOM, with *DS* of 3.0 differes substantially from that of cellulose acetate, being ca. 20% lower for the former than for the latter. The reason for a considerable lowering of AC% can be ascribed to the introduction of oligo-oxymethylene groups $-(CH_2O)_s-$ bonded between glucopyranose ring and acyl group in the side chain. Based on this difference in AC% between cellulose acetate and CAcOM whose *DS* values are both estimated to be 3.0, the number of oxymethylene unit *s* introduced in the side chain-molecular substitution-can be calculated. Table 4-1 shows the relationship between dissolution condition (time and temperature) of cellulose and *s* determined from CAcOM. It can be seen that the values of *s*, which indicate the measure of the oxymethylene chain length increase from 1.2 to 2.2 in order of dissolution condition A, B, C, and D.

Table 4-1. Dissolution condition of cellulose

Dissolution condition of cellulose			
Temperature (°C)	Time (min)	*s* in $-(CH_2O)_s-$	Symbol
120	180	1.2	A
120	80	1.8	B
120	25	2.0	C
110	35	2.2	D

The conditions B and C were adopted only for (cellulose oligo-oxymethylene ether) acetate.

4.2 Change in tensile properties with oxymethylene chain length

In Chapter 3, I studied the tensile properties of COAs from acetate to valerate, and found that by increasing the number of carbons, *n*, in the acyl side chain, mechanical properties of COAs shifted from a strong and tough type to an elastomeric one. On the other hand, since each chain of COAs consists of both the acyl and oxymethylene portions, i.e. $-(CH_2O)_s$-COR, the tensile properties of COAs may also be affected when the side chain varies at the oxymethylene portion instead of acyl portion. Figure 4-1 shows the stress-strain diagrams of CAcOM (A, B, C, and D) in tension measured at 20°C and 65% R.H. Symbols used in parenthesis hereinafter indicate dissolution condition mentioned above. These diagrams are similar in shape, and have an yield point. However, as *s* in the oxymethylene part increases, the Young's modulus and an yield strength decrease while maximum elongation increases. This trend corresponds to that observed for COAs when *n* increased from 2 to 5 in the acyl group portion (See 3.3). From

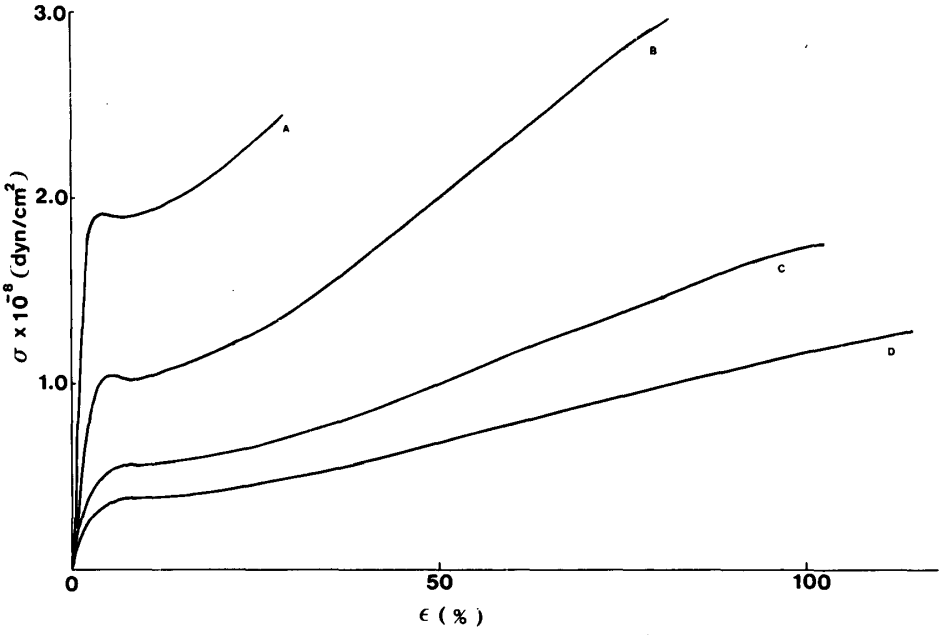

Fig. 4-1. Stress-strain diagrams of CAcOM (A, B, C and D).

these results, it is known that changing length of the oxymethylene or acyl chains gives similar effect to the tensile properties of COAs despite their difference in molecular structure. In this connection, it can be noted that the stress-strain diagrams were obtained in the temperature region of the β process for CAcOM. Thus, there exists an intimate relation between the molecular motion in the β process and the stress-strain curves examined. Therefore, the results of the stress-strain diagrams obtained above suggest that the motion of the oxymethylene chain may also be related to the β process, though the process is known to involve the motion of acyl chain. This point is discussed and confirmed later on the basis of the results of dynamic mechanical measurements.

4.3 Effect of oxymethylene chain length on the relaxation processes of the acetate

Figures 4-2a and 4-2b respectively show the variation of dynamic modulus E' and loss modulus E'' with temperature for CAcOM (A, B, C, and D). In the figures, the result for cellulose acetate is also included as a special case of CAcOM wherein the value of s is zero. With respect to E'', three relaxation processes were observed for both cellulose acetate and four kinds of CAcOM within the experimental frequency and temperature ranges. They are labelled α_m, β_m, and β'_m for cellulose acetate in order of decreasing temperature at which they were detected.

According to the early works for the mechanical relaxation processes of cellulose acetate[22], the α_m and β_m processes are respectively due to the micro-Brownian

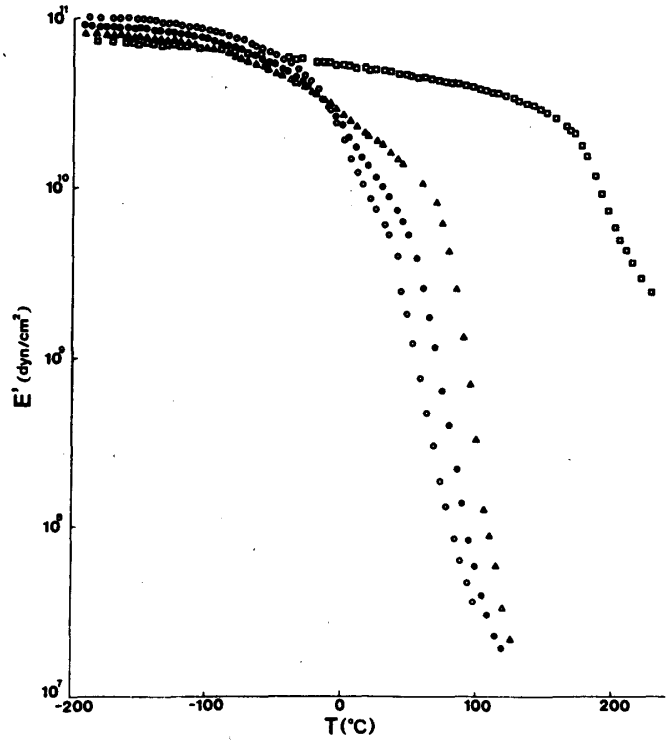

Fig. 4-2a. Temperature dependence of dynamic modulus E' for CAcOM (A, B, C, and D) and cellulose acetate. CAcOM (A): △, (B): ●, (C) and (D): ○, cellulose acetate: □.

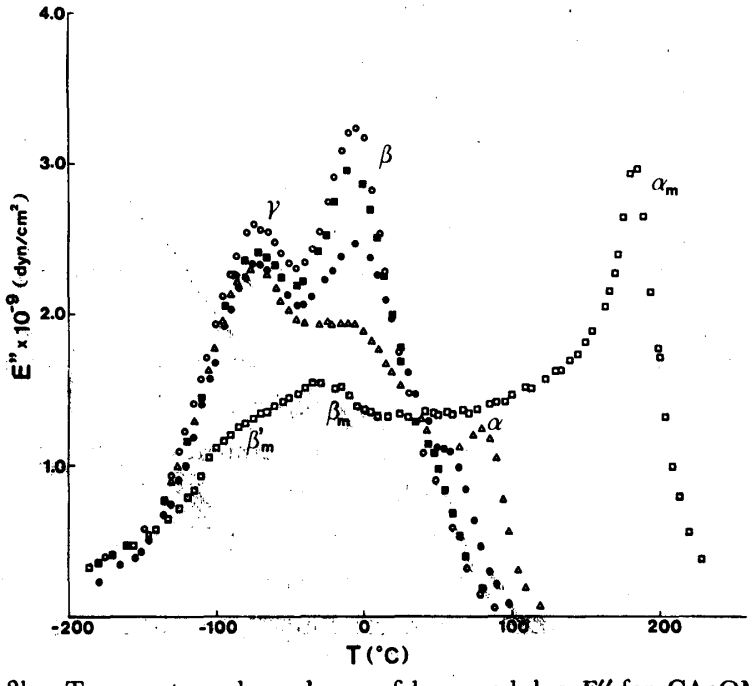

Fig. 4-2b. Temperature dependence of loss modulus E'' for CAcOM (A, B, C, and D) and cellulose acetate. CAcOM (A): △, (B): ●, (C): ■, and (D): ○, cellulose acetate: □.

motion of the segment along the main chain and the motion including the acetate group in the side chain. This is consistent with the results for other acylates described in Chapter 1. In addition, in Chapter 1, the apparent activation energy ΔE for the α_m process was estimated to be more than 50 kcal/mol, while that for the β_m process to be less than 8 kcal/mol. Although these two processes were also observed by using dielectlic measurements in the corresponding frequency and temperature regions, the β'_m process could not be detected within the range examined (see Chapter 2). The β'_m process may be due to the local side chain motion around C-5 and C-6 axis of a glucopyranose ring. The α_m process will be discussed in the later section in relation to the α process.

On the other hand, CAcOM from A to D exhibits quite different relaxation processes from those for cellulose acetate. Concerning the γ process in the Figure 4-2b, the maximum E'' value seems to increase as s increases, even if the influence of the β process is subtracted in E''-temperature curves. The same results are also observed in this region for the other homologues of COAs as examplified for (cellulose oligo-oxymethylene ether) valerate, CVaOM and hexanoate, CHeOM in Figures 4-3 and 4-4, respectively. This process has been considered to be the motion of the oxymethylene group in the side chain from the results of the dielectric measurements. If this is the case, the γ peak should increase in height as s increases, because in general the increase in the number of the motional unit responsible for the relaxation process noted causes increased peak height for

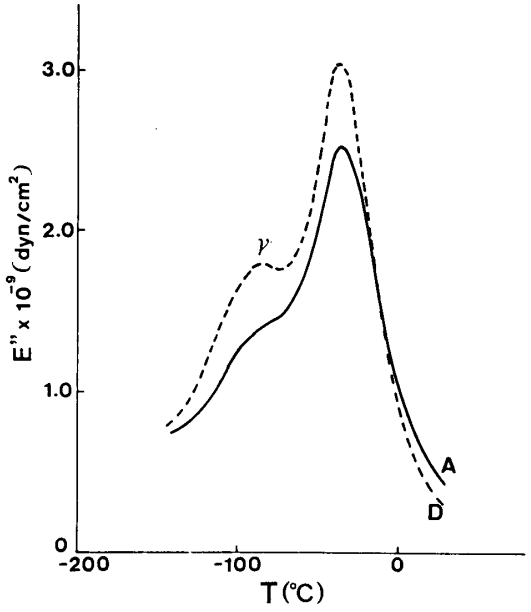

Fig. 4-3. Temperature dependence of loss modulus E'' for CVaOM (A and D).

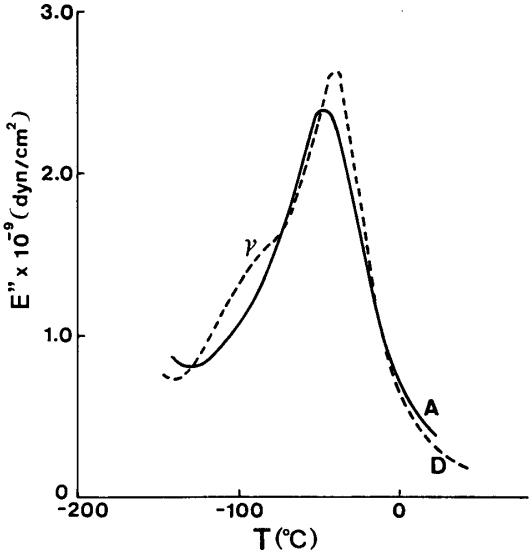

Fig. 4-4. Temperature dependence of loss modulus E'' for CHeOM (A and D).

polymers in the glassy state. Accordingly, from the results shown in Figures 4-2, 4-3, and 4-4 the γ process is confirmed to be due to the motion of the oligo-oxymethylene group in the side chain.

The β process has been assigned to be due to the motion involving acyl side chain, since the process was largely affected by n. As shown in Figures 4-2a and 4-2b, however, both the maximum E'' values and the relaxation magnitude in the β region increase markedly also with increasing s. Hence, the β process is considered to include not only the motion of the acyl parts but also that of the oligo-oxymuthylene parts in the side chain. For further information on the β process, note the E'-temperature curves for COAs. The change in E' for COA in the glassy state when s increased is quite different from that when n increased. As shown in Figure 4-2a, E'-temperature curves for CAcOM along with cellulose acetate intersect at the temperature in the neighbourhood of the β region: with increasing s, E' values in the temperature range below the intersecting point increase, while they decrease above the point. The same results were also observed for other homologues of COAs when s increased. The reason for a rise in E' with s in the region below the β peak temperature can be ascribed to the increased interchain cohesive force resulting from the increased contents of polar oxymethylene groups. On the other hand, because changing length of the acyl or oxymethylene chains gives similar effect on the E' above the β region, the molecular motion of the oxymethylene chain is considered to be released enough to randomize their dipole orientation within the time scale observed, causing decreased interchain cohesive force. From these findings and discussion, the β proces is concluded to be due to the segmental motion along the side chain which includes both the oxymethylene and acyl chains, i.e., $-(CH_2O)_s$-COR.

4.4 The effect of oxymethylene chain length on the glass transition temperature of the acetate

In addition to the processes discussed above, the α process for COAs and α_m process for cellulose acylates are observed in higher temperature range as shown in Figure 4-2b for CAcOM and cellulose acetate. These processes have been regarded as due to the micro-Brownian motion of the main chain, and thus a considerable drop in E' in the corresponding region in Figure 4-2b is related to the glass rubber transition of the polymer. Therefore, the temperature location of E'' maximum in the α and α_m regions measured at such a low frequency as 110 Hz can be regarded as a rough measure of the glass transition point T_g of the samples. For cellulose acetate, T_g thus defined is located at about 180°C, while for CAcOM it appears considerably lower temperatures below 100°C. Furthermore, it can be seen that T_g of CAcOM moves to lower temperatures with increasing s.

The similar results were also recognized for other COAs. One should remind here that in Chapter 3 (Section 4) the lowering of T_g was also observed for COAs when n increased. Because the polar oxymethylee group introduced in COAs plays a similar role to that of non-polar alkyl group on the β process, its influence to the subsequent α process must be similar. Therefore, the reason for a lowering of T_g with increasing s from 0 to 2.2, can be interpreted in the same manner as the lowering of T_g with n: the introduction of the oxymethylene groups induces increased separateon of each main chain, and additional introduction of the oxymethylene groups facilitate further separation of each main chain, resulting in a weakening of interchain cohesive force which causes a lowering of T_g.

4.5 Comparison of glass transition temperature among the cellulose derivatives and synthetic polymers

As was seen above, each process for COAs is largely affected by the change in length of the oxymethylene chain in the side chain in the same manner as that induced by the change in n, when the length of the acyl chain is short as in CAcOM. However, if the length of the acyl chain in COAs is long enough as compared to that of the oxymethylene chain, the effect of the variation of s on each process may become small, because in such a case the ratio of the length of the oxymethylene chain to that of the side chain is small. Therefore, it is of interest to note whether or not the relaxation processes for COAs having large n are affected by the variation of s. For elucidating this point, I note the influence of the oxymethylene chain length to the temperature location of the α process, i.e., T_g for COAs.

Figure 4-5 shows the diagrams of T_g values determined from tan δ maximum versus n for a series of COAs (A, and D) and cellulose acylates. In the figure, the results for a series of polyalkylmethacrylates is also quoted for reference. At $n=2$, the difference in T_g with s among COAs (A), (D), and cellulose acylate is very large, while it decreases markedly as n increases, and finally little difference in T_g is observed at $n=10$. Consequently, it follows that T_g of COAs with large n do not vary in a great extent with the length of the oxymethylene chain within the range examined. In this connection, it should be noted that T_g reduction for both COAs and cellulose acylates levels off above room temperature. On the other hand, from the results in Chapter 5 cellulose derivatives having linear and flexible side chain are shown to exhibit lower T_g values than those of cellulose derivatives with bulkier side chain, when their molecular weight is the same as far as the side chain portion is concerned. Therefore, based on the finding that even the cellulose derivatives with linear and flexible side chain exhibit a lower limit of T_g above room temperature, it is suggested that all the cellulose derivatives

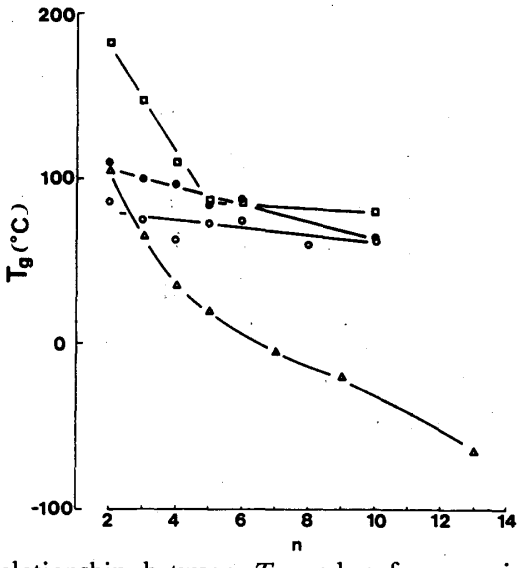

Fig. 4-5. Relationship between T_g and n for a series of COAs (A and D), cellulose acylates and polyalkylmethacrylates. CAcOM (A): ●, CAcOM (D): ○, cellulose acylates: □, polyalkylmethacrylates: △.

have a lower limit of T_g above room temperature. In contrast, the lowering of T_g for polyalkylmethacrylates proceeds quite different manner from that for COA as shown in the figure. In this series, T_g decreases with increasing n, showing no levelling off. The difference between cellulose derivatives examined here and poly-*n*-alkyl methacrylates, both having linear and flexible side chain, may be attributed to the different structure of the main chain: the former is bulkier than the latter.

4. 6 Contribution of oxymethylene portion to the β and γ processes of COAs

The extent of the contribution of the oxymethylene chain to the relaxation processes for COAs is more directly reflected to the β and γ processes in the glassy state because they are related to the motion involving oxymethylene chain itself. Figure 4-6 illustrates the plots of E'' with linear, arbiterary scale against temperature for a series of COA (D) from $n=2$ to 10 in the temperature range from −190°C to 100°C. It can be seen that even when the n increases, the γ region, caused from the motion of the oxymethylene portion, remains at a constant temperature of about −70°C, though the neighbouring β region shifts to lower temperature. Furthermore, the γ peak which is clearly visible for COA with $n=2$ become less distinct, and finally for COA with $n=10$, i.e., (cellulose oligo-oxymethylene ether) decanoate, CDeOM, it merged completely in the low temperature tail of the β peak. On the other hand, the additional δ process is seen to appear below −160°C for COA above $n=4$. However, this process is not related to the molecular motion in the oxymethylene portion, since it is considered to be the

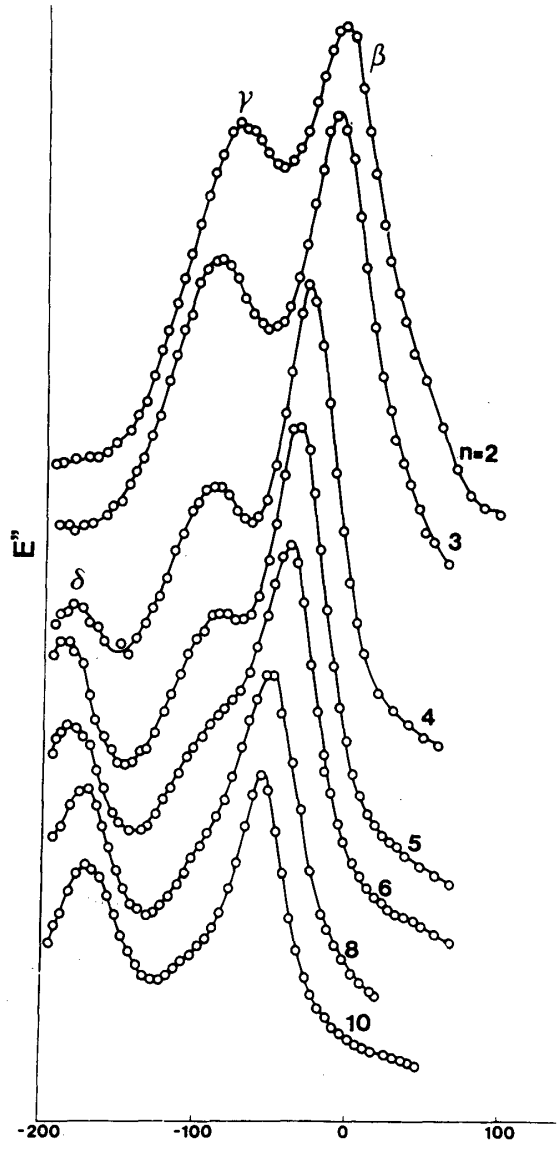

Fig. 4-6. Temperature dependence of loss modulus E'' for a series of COAs (D) from $n=2$ to 10.

motion of three or more methylene groups in a row in the side chain, and, at this temperature, the oxymethylene portion is in the freezed state. From these results, viscoelastic properties of COA with large n is expected to be almost unaffected by the values of s.

4.7 The similarity in the viscoelastic properties among cellulose acylates and COAs

Figures 4-7a and 4-7b show the variation of E' and E'', respectively, for CDeOM (A, D) and cellulose decanoate whose n values are the largest in the series examined. As is expected, all the relaxation processes appearing in both CDeOM (A) and CDeOM (D) seem similar despite their different s values.

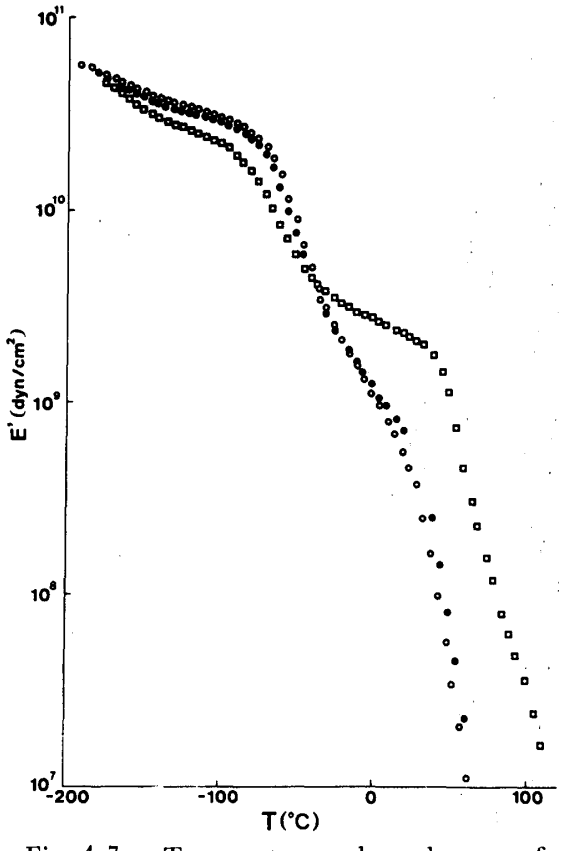

Fig. 4-7a. Temperature dependence of dynamic modulus E' for CDeM (A, D) and cellulose decanoate. CDeOM (A): ●, (D): ○ cellulose decanoate: □.

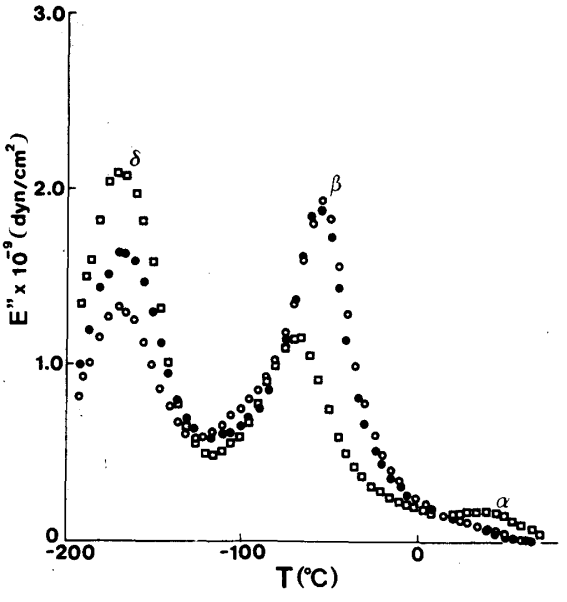

Fig. 4-7b. Temperature dependence of loss modulus E'' for CDeOM (A, D) and cellulose decanoate. CDeOM (A): ●, (D): ○, cellulose decanoate: □.

Furthermore, it should be noted that this similarity is also recognized in the relaxation processes for CDeOM (A, D) and cellulose decanoate which lacks the oxymethylene portion in the side chain. From this result, it is concluded that the role of the oxymethylene group to the relaxation mechanism of COAs becomes negligibly small for large n.

5. Effect of bulky side chain on the relaxation process of COAs

As shown in the previous two chapters, the COAs series are characterized by observing that the micro-Brownian motion in the side chain (β process) appears separately from that in the main chain (α process). The existence of the two kinds of micro-Brownian motion is considered to be a result of the difference in flexibility between the side chain and the main chain: the former consists of the smaller and more flexible motional unit such as $-CH_2-$ or $-O-$ than the latter, i.e., glucopyranose ring. If this is the case, a COA should exist without the β process. In that case side chains would involve such bulky motional unit as glucopyranose

rings.

This chapter describes viscoelastic properties of newly prepared COAs with acyl side chain bulky in chemical structure (iso-butyrate, pivalate, and benzoate), in relation to those of COAs with linear acyl group, using dynamic mechanical measurements[48]. All the COAs prepared gave clear, transparent films.

5.1 Melting and glass transition

Thermal analysis using TMA gives useful information on glass transition or melting of polymer samples as described in Chapter 3. One of the resulting diagrams of thermal deformation (***D***) versus temperature is illustrated in Figure 5-1 for (cellulose oligo-oxymethylene ether) pivalate, CPiOM. All the COAs examined gave a deformation thermodiagram pattern similar to that for CPiOM, showing two transition regions above room temperature.

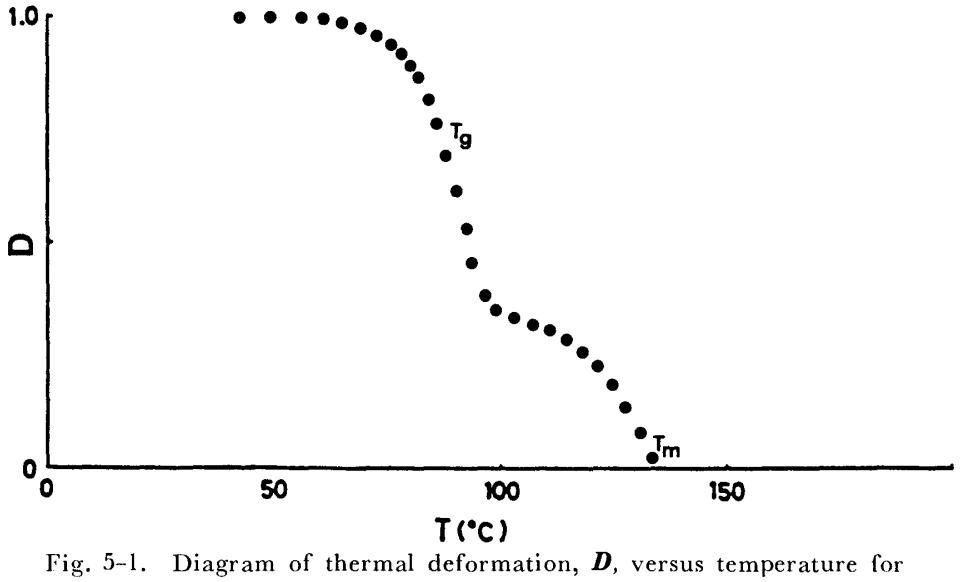

Fig. 5-1. Diagram of thermal deformation, ***D***, versus temperature for (Cellulose oligo-oxymethylene ether) pivalate, CPiOM.

Figure 5-1 shows that the higher temperature range transition proceeds gradually prior to melting of the sample. In contrast, highly crystalline polymers are known to exhibit a well-defined transition point from solid to liquid state in the thermodiagram[49]. Because all the COAs examined do not exhibit such a well-defined transition point in the thermodiagram just before melting, they are considered to be amorphous in nature. This is consistent with the results of X-ray diffraction measurements mentioned in Chapter 3 (Section 2).

On the basis of the results in Chapter 3 (Section 1), the lower temperature range transition can be attributed to the segmental motion of the main chain, i.e., micro-Brownian motion (α process). Thus, the temperature corresponding to the

Table 5-1. Glass transition point T_g and apparent melting point T_m for COAs.

Samples	T_g (°C)	T_m (°C)
CAcOM	83	164
CBuOM	65	121
CVaOM	49	114
CiBOM	74	143
CPiOM	90	136
CBzOM	88	190

dD/dE maximum in the region can be regarded as about equal to the glass transition point T_g of the sample. Table 5-1 shows T_g along with T_m for six kinds of COAs examined in the present work. It can be seen that the values of T_g for COA with linear side chain decreases regularly with increasing molecular weight of the side chain: 83, 65, and 49°C for (cellulose oligo-oxymethylene ether) acetate (CAcOM), butyrate (CBuOM), and valerate (CVaOM), respectively. The change of T_m shows a similar trend. However, as was observed in early work for polyalkyl methacrylate or acrylate with bulky side chain[50], such regularity in T_g disappears when the molecular weight of the side chain increases by introducing bulky acyl group in the order of acetate, iso-butyrate, pivalate, and benzoate. In this case, the lowest T_g value of the four is given in (cellulose oligo-oxymethylene ether) iso-butyrate, CiBOM, while the highest T_m for (cellulose oligo-oxymethylene ether) benzoate, CBzOM.

In the following, the dynamic mechanical properties of COAs with bulky side chain (CiBOM, CPiOM, and CBzOM) are compared to those of COAs having linear side chain with a corresponding molecular weight.

5.2 Comparison of dynamic mechanical properties between the butyrate and iso-butyrate

Figures 5-2 shows the dynamic modulus E' and loss modulus E'' at 110 Hz as a function of temperature for both CBuOM and CiBOM. Regarding E''-temperature curves, CiBOM reveals three processes above −150°C, each of which is considered to be similar in molecular mechanism to the corresponding processes in CBuOM. These can also be labelled α, β, and γ, respectively. The γ peak for CiBOM is located at the same temperature as that for CBuOM, while both the β and α peaks for CiBOM shift to higher temperatures as compared to CBuOM. Since the motion of the oligo-oxymethylene portion is responsible for the γ process as described in Chapters 3 an 4, this data shows the kind of acyl group has little effect on temperature-frequency locations of the γ process.

The β process, however, is initiated by the micro-Brownian motion of the side

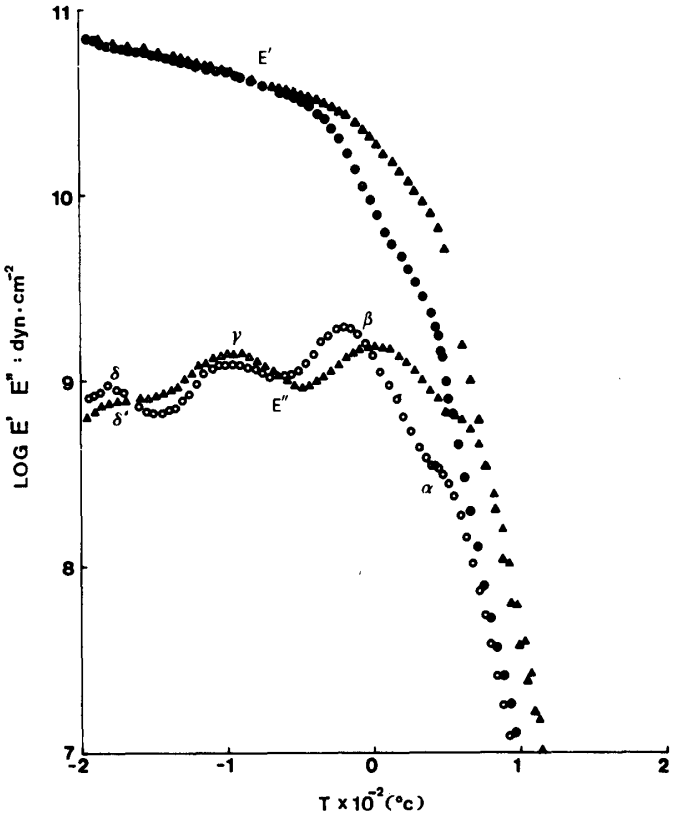

Fig. 5-2. Temperature dependence of dynamic modulus E', loss modulus E'' at 110 Hz for (Cellulose oligo-oxymethylene ether) butyrate, CBuOM, ○, ● and iso-butyrate, CiBOM △, ▲.

chain (See 4.3). The high temperature shift of this region for CiBOM is thought to cause decreased mobility of the segment along the side chain. This comes from an increase in steric hindrance of the bulky iso-butyrate group as compared with that of the linear butyryl group.

Comparing the relaxation magnitude in the β region for CiBOM with that for CBuOM in E'-temperature curve, it follows that the lowering of the side chain mobility for CiBOM results in the decreased relaxation magnitude. Both the COAs reveal the same E' value at temperatures below the β region. It can be further observed that the α region for CiBOM shifts to highr temperature, indicating that the mobility of the side chain affects that of the main chain.

In addition to these three processes (α, β, and γ) commonly observed for both the COAs, CBuOM exhibits an additional process labelled δ below -150°C. The δ process has been thought to arise from the twisting motion involving at least three or more methylene groups in a row in the side chain (See 3.6). The E''-temperature curve for CiBOM reveals a relaxation process (labeled δ') as a shoulder in the region comparable to that of the δ process for CBuOM, though

CiBOM lacks $-CH_2-CH_2-CH_2-$ parts. On the basis of the corresponding findings concerning polymers in a series of cellulose acylates (Chapters 1 and 2), the δ' process can be assigned to the motion initiated by $-CH_2-CH_2-$ parts in the side chain.

5. 3 Comparison of dynamic mechanical properties between the valerate and pivalate

The difference observed in the relaxation process between CBuOM and CiBOM becomes even greater when comparisons are made between CVaOM and CPiOM. In these, acyl parts in the side chain have greater molecular weight than CBuOM or CiBOM. Figure 5-3 shows the dynamic modulus E' and loss modulus E'' at 110 Hz against temperature for both CVaOM and CPiOM.

Concerning E' values, CPiOM has lower E' values in the range below $-50°C$ than those of CVaOM. This lowering in E' is not observed when the butyryl group is in place of the isobutyryl groups in the side chain (Figure 5-2). The introduction of a bulky acyl side chain (pivalate) substantially reduces interchain cohensive force in COA as compared with that in COA having linear side chain

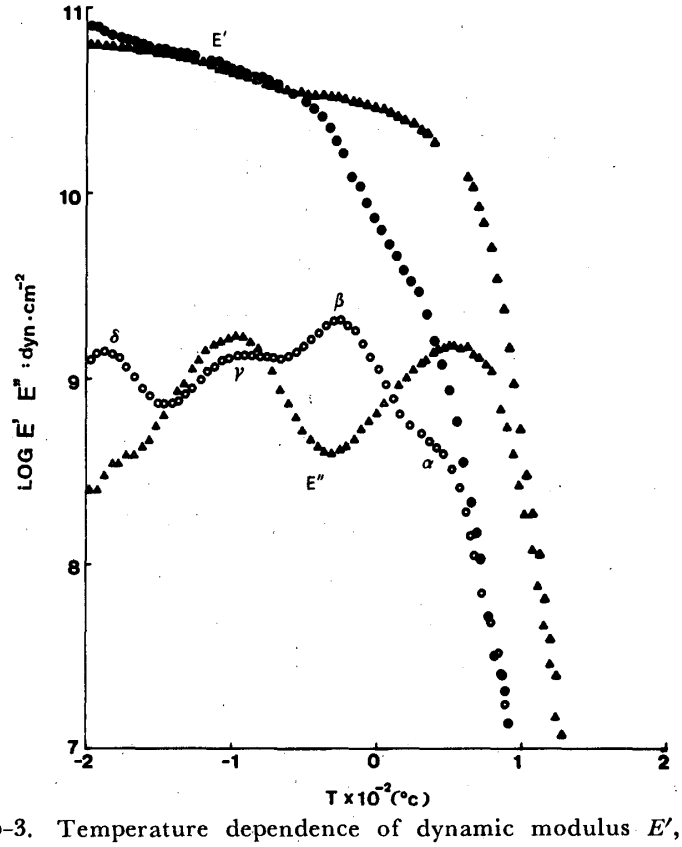

Fig. 5-3. Temperature dependence of dynamic modulus E', loss modulus E'' at 110 Hz for (Cellulose oligo-oxymethylene ether) valerate, CVaOM, ○, ● and pivalate, CPiOM △, ▲.

of equal molecular weight.

With respect to E'', the two curves are quite different in shape except for those in the γ region. At about $-180°C$, the δ process clearly observed for CVaOM disappears for CPiOM because of the absence of $-CH_2-CH_2-CH_2-$ parts in the side chain. While CiBOM do not exhibit the δ process because of lacking $-CH_2-CH_2-CH_2-$ parts, it shows the δ' process due to the motion of $-CH_2-CH_2-$ parts in the side chain. This indicates that for CPiOM, even the twisting of $-CH_2-CH_2-$ parts does not occur because of the steric hindrance caused by $-CH_3$ branch around $-CH_2-CH_2-$ parts within the pivalate group.

In the temperature regin of the overlapping β and γ processes for CVaOM, CPiOM shows one distinct process. From its temperature-frequency locations, I assign it to the γ process. In Chapter 3 (Section 7), because of the overlapping of the γ region to the β region in COAs with linear side chain, I determind the apparent activation energy ΔE for the γ process from its resolved E''-temperature curve. This has been done by assuming that both γ and β have Gaussian distribution. As is seen in Figure 5-3, however, the γ peak for CPiOM is distinct without any influence of other processes. Thus, the ΔE value for the γ process can be estimated more precisely for CPiOM than for other COAs, being 10.5 and 10.1 kcal/mol from E' and tan δ curves, respectively.

A broad-shaped peak for CPiOM is observed in the higher temperature range. For elucidating the relaxation mechanism in this region, variation of

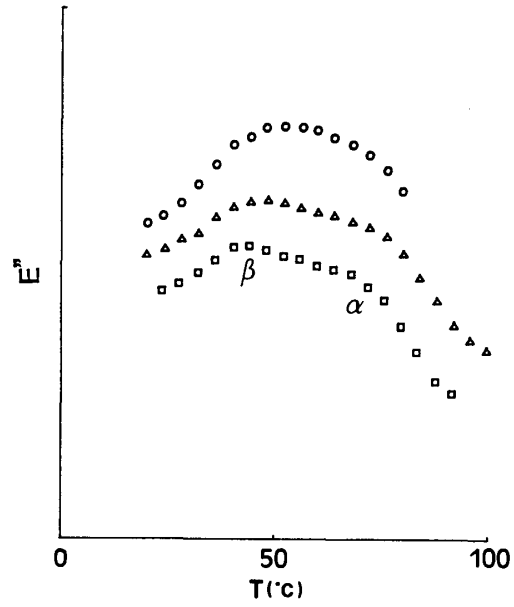

Fig. 5-4. Variation of E'' temperature curve with frequency for (Cellulose oligo-oxymethylene ether) pivalate, CPiOM. ○: 110, △: 35, □: 11 Hz.

E''-temperature curves for CPiOM with frequency are shown in Figure 5-4. The broad-shaped peak obtained at 110 Hz shows some splitting when lower frequency is used for the measurement, indicating the existence of the two kinds of processes in the range noted. Because the shoulder at about 70°C in a curve measured at 11 Hz corresponds to the glass transition region, this process can be regarded as the α process. Because the mobility of the bulky pivalate group is considered to be reduced by its steric hindrance compared with that of the valarate group, the β region shifts markedly to the higher temperature, and appears slightly below the α region. The process just below the α region can be classified as the β process for CPiOM. It is also found that for CPiOM, the α region moves to higher temperature with the high temperature shift of the β region.

5. 4 Dynamic mechanical properties of the benzoate

When the bulky acyl group is changed from iso-butyrate to larger pivalate, a bigger shift of the β region occur toward the higher temperature as compared to that of the α region. This indicates the mobility of the side chain segment approaches that of the main chain segment. Thus, it is expected that if the bulky

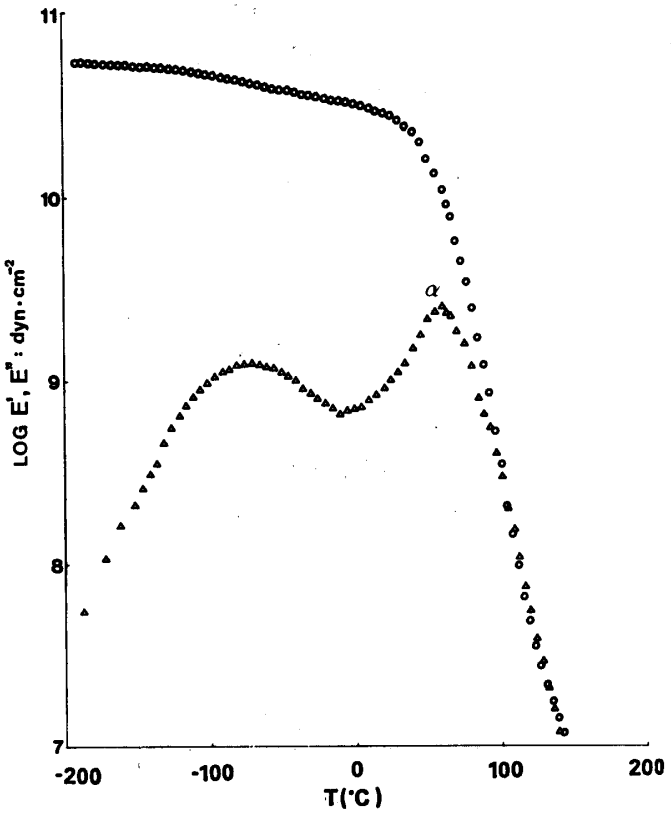

Fig. 5-5. Temperature dependence of dynamic modulus E'' and loss modulus E'' at 110 Hz for (Cellulose oligo-oxymethylene ether) benzoate. CBzOM.

acyl group in the side chain of COA were large enough (i.e. glucopyranose ring or benzene ring) the mobility of the segment in the side chain would be reduced and become similar to that in the main chain. This would result in the extinction of the β process.

To examine this point, Figure 5-5 displays the variation of E' and E'' at 110 Hz with temperature for CBzOM where the acyl portion in the side chain involves benzene ring. The figure shows that two processes occur. The process appearing at about 70°C is sharp in contrast to the corresponding process for CPiOM. In this region, E' values decrease markedly from 2.05×10^{10} dyn/cm^2 to less than 10^7 dyn/cm^2 as the temperature rises from 40°C to 140°C. Furthermore, ΔE values for this process calculated from E'' and tan δ curves are respectively 53.5 and 55.3 kcal/mol. From these findings, the process can be regarded as a micro-Brownian motion along the main chain (α process). It should be emphasized that the β process having been observed for all other COAs examined disappears for CBzOM. Accordingly, I conclude that for CBzOM, the micro-Brownian motion along the side chain, independent of that along the main chain, cannot appear in the diagram because of the similarity in the molecular size of both the benzene ring in the side chain and glucopyranose ring in the main chain.

In addition to the α process, the γ process (due to the motion of the oxymethylene portion) should appear at about -100°C at 110 Hz regardless of whether the acyl group in the side chain is bulky or not. As is seen in Figure 5-5, however, the temperature location of the process detectd in the lower temperature apparently differs from that of the γ process for other COAs. This discrepancy can be interpreted by considering the existence of an additional process in the

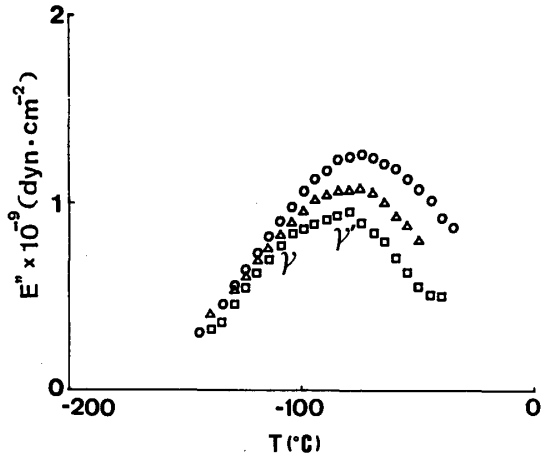

Fig. 5-6. Variation of E'' temperature curve with frequency for (Cellulose oligo-oxymethylene ether) benzoate, CBzOM. ○: 110, △: 35, □: 11 Hz.

vicinity of the γ process.

Figure 5-6 illustrates the variation of E''-temperature curves for CBzOM with frequency at temperatures between −150°C and −20°C. From the plots at 11 Hz, two processes are clearly recognized. The process at the lower temperature can be ascribed to the γ process because of its location. The process at the higher temperature (which is labelled γ') may correspond to the motion involving benzyl groups which was observed in benzyl cellulose in the corresponding region[51].

PART III Novel Cyanoethylated Cellulose

6. Cyanoethylated cellulose prepared by homogeneous reactin in PF/DMSO system

Cyanoethylation of cellulose can be traced back to the pioneering work of MacGregor et al.[52] in the 1940s. Since then, partial cyanoethylation of cotton cellulose has been extensively studied to improve its duarabilities, such as thermal, chemical, and microbiological resistance[53]. The other cellulosic materials have also been cyanoethylated to obtain a highly substituted product[54], which was used as an electric material because of its high dielectric constant, although it is brittle in nature.

While these reactions proceed heterogeneously, a homogeneous cyanoethylation reaction of cellulose in viscose medium is also known[52]. However, in this case, the degree of substitution seldom reaches 2.0, due to the steric hindrance of xantate groups introduced to cellulose, and no notable products were expected from this method for the practical use.

In this chapter, the homogeneous cyanoethylation method for cellulose is presented as the other application of PF/DMSO solvent[55]. The physical properties of the resulting products differ substantially from those of the cyanoethylated cellulose prepared by the traditional method. For example, although the traditional products are not available for film application due to their brittle nature, the products prepared in PF/DMSO medium give clear, transparent and flexible films which suggests the possibility of these products being applicable to various new fields.

The detailed procedure for preparing cellulose solution was described in Chapter 3. Dried cellulose powder (6 g) and PF (12 g) dispersed in DMSO (150 ml) were stirred generously at 120°C for 80 min. The resulting transparent solution was cooled to room temperature and left. To the cellulose solution thus obtained was added specified amount of Na/DMSO solution in which sodium metal (0.19 g) was dissolved in DMSO (50 ml), then was added acryronitrile (30 ml). The reaction mixture was kept at room temperature for 24 hr with continuous

stirring, after which it was poured into excess methanol to obtain the products. In some cases, the reaction mixture before pouring was divided into two parts, in which one was poured into excess methanol as described just above, while another was followed by acetylation reaction. In another case, an attempt was made to obtain a cyanoethylated sample by using a traditional method as a reference. Cellulose powder was immersed in a weak (3%) aqueous solution of sodium hydroxide, squeezed free of excess liquor, treated with excess acrylonitrile at 50°C for several hours, and then poured into excess water to yield products.

6.1 Infrared spectra of the samples prepared

Figure 6-1 shows the infrared spectra of the products prepared by homogeneous reaction in PF/DMSO solvent system. From the absorption bands at 2,950, 2,250, 1,480, 1,420, 1,370, 1,330, 1,270, and 1,230 cm^{-1}, it appears that the cellulose are cyanoethylated. By increasing the amount of Na/DMSO added to the system, the intensity of these absorption bands due to cyanoethyl groups increase, while that of OH absorption at around 3,450 cm^{-1} decreases. From this, it was found that

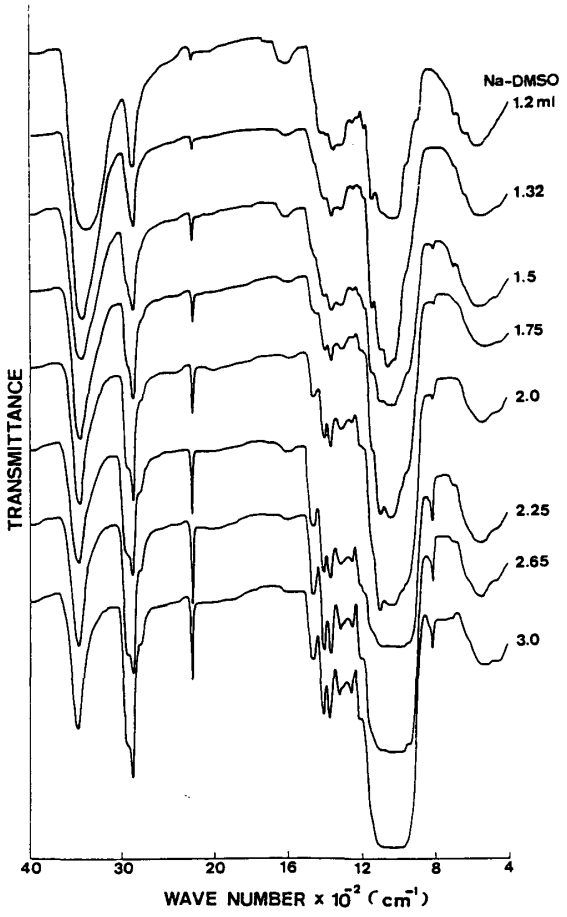

Fig. 6-1. Infrared spectra of the cyanoethylated cellulose prepared in PF/DMSO medium.

the degree of cyanoethylation proceeds in the order of the amount of Na/DMSO. However, even if an additional amount of Na/DMSO (3.0 ml or more) is added, the intensity of above bands remains fairly constant. In this connection, it is known that the infrared spectra of cyanoethylated cellulose prepared by the conventional method often exhibit additional absorption bands due to carbamyl or carboxyethyl groups which are introduced by side reactions. However, since there is no such evidence in all spectra shown in Figure 6-1, cyanoethylation method in this study can be regarded as more effective than the conventional method.

For a qualitative analysis concerning the degree of cyanoethylation, one should note the absorbance ratio of A_{CH} at 2,900 cm^{-1} to A_{OH} at 3,450 cm^{-1}, i.e. A_{CH}/A_{OH}. Brown et al.[55] studied infrared spectra of a series of cyanoethylated cellulose with various degree of substitution (*DS*), which is prepared by homogeneous reaction in viscose, and reported that the product with $DS=0.77$ in the series is soluble in water. The A_{CH}/A_{OH} value of this product was 0.5. It is noted that auther's cyanoethylated cellulose with $A_{CH}/A_{OH}=0.36$ obtained in case of Na/DMSO=1.32 ml is also water soluble. So far water-soluble cyanoethylated cellulose has been known to be prepared only by homogeneous reaction in viscose. Therefore, auther's method suggests a new way to prepare a water-soluble cyanoethylated cellulose. On the other hand, highly cyanoethylated cellulose (Na/DMSO=3.0 ml) obtained by auther's method is soluble in dry acetone in the same manner as the conventional cyanoethylated cellulose whose *DS* value is 2.5 or more. Judging from high solubility in acetone and high A_{CH}/A_{OH} value, *DS* value of the highly cyanoethylated cellulose prepared by auther's method is expected to be about 2.5. This will be discussed again and confirmed in the last paragraph of this chapter.

6.2 Chemical structure of newly prepared cyanoethylated cellulose

The degree of modification of cyanoethylated cellulose is usually expressed by nitrogen content. Figure 6-2 shows a relationship between the percentage of nitrogen contents (*%N*) and A_{CH}/A_{OH} value for auther's cyanoethylated cellulose. In the figure, the result of cyanoethylated cellulose prepared by a reaction in aqueous medium (hereinafter termed as conventional CEC) is also included. It can be seen that, with increasing the value of A_{CH}/A_{OH} up to ca. 1.2, nitrogen contents increase, while it levels off for A_{CH}/A_{OH} above 1.2. It should be noted here that the plot for conventional CEC greatly deviates from the regression curve shown in the figure: the nitrogen contents of conventional CEC at $A_{CH}/A_{OH}=1.36$ is measured to be 11.3%, though 7.9% is expected from the curve. This discrepancy becomes clearer by converting the nitrogen contents of 7.9 and 11.3% into the corresponding *DS* value of 1.3 and 2.3, respectively, on the basis of a well-known conversion formula, i.e.,

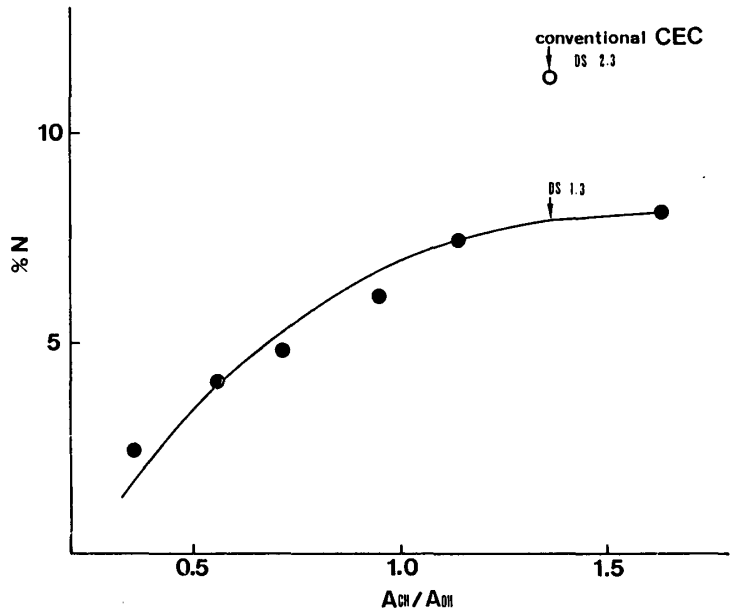

Fig. 6-2. Relationship between percentage of nitrogen contents ($\%N$) in the cyanoethylated cellulose and the ratio of absorbance A_{CH} at 2,900 cm^{-1} to A_{OH} at 3,500 cm^{-1} (A_{CH}/A_{OH}).

$$DS=(162\times\%N)/(1,400-53\times\%N).$$

From these findings, it is suggested that a newly prepared cyanoethylated cellulose may be different in chemical composition from the conventional cyanoethylated cellulose, despite the similarity of their infrared spectra.

6.3 Thermal deformation properties

Figure 6-3 shows the diagrams of thermal deformation ***D*** in arbitrary scale against demperature with auther's cyanoethylated cellulose having various degrees of cyanoethylation, Whatman cellulose CF-11, and the regenerated cellulose from PF/DMSO system. The thermodiagrams labelled A to G correspond to the infrared spectra in Figure 6-1 in case of Na/DMSO=1.2, 1.32, 1.75, 2.0, 2.25, and 3.0, respectively. The absorption ratio, A_{CH}/A_{OH}, is also shown in the Figure for reference. For the Whatman cellulose, the deformation due to carbonization of the sample occurs at around 330°C, while for the regenerated cellulose it appears at a temperature 30°C lower than that for the Whatman cellulose. This lowering may be attributed to the decreased amount of the crystalline region in cellulose. The similar diagram to that of the regenerated cellulose was observed for the sample A, in which the trace amount of cyanoethyl groups was introduced in the side chain. Further cyanoethylation induced different thermal properties from those of cellulose. For the sample B which is soluble in water as mentioned before, two transition regions were recognized. The first region appeared at temperatures bet ween 0°C and 100°C, then the second region above 100°C, and finally the

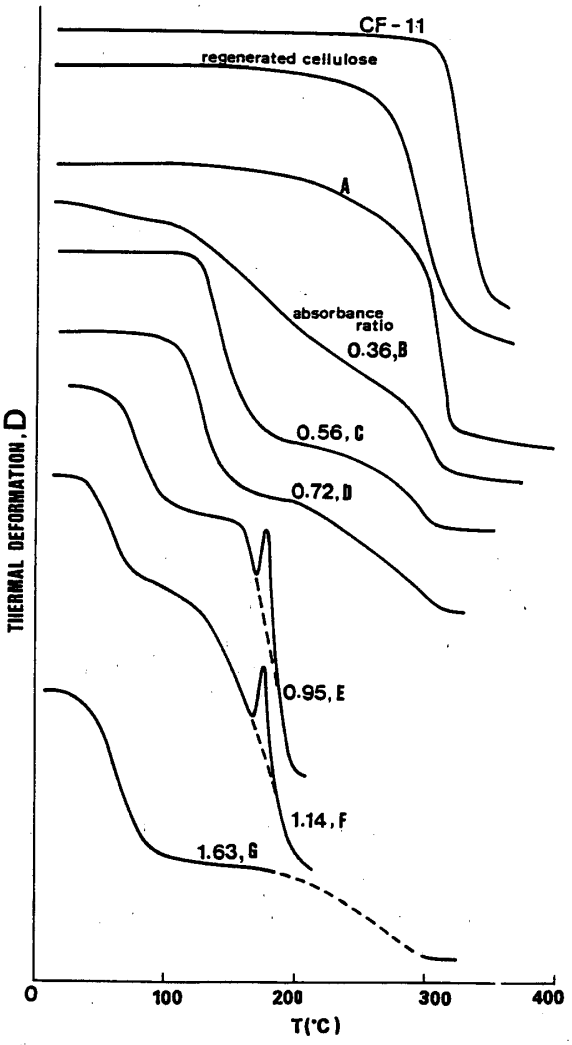

Fig. 6-3. Digraam of thermal deformation D in arbitrary scale versus temperature for Whatman cellulose CF-11, regenerated cellulose and cyanoethylated cellulose.

carbonization process occurred at about 300°C. For the sample C, the deformation diagram exhibits a remarkable transition at around 120°C prior to the carbonization. Similar transitions were also seen for cyanoethylated cellulose from D to G. Since cyanoethylated cellulose is known to be amorphous in nature, this transition can be regarded as due to the glass-rubber transition of the sample. In this region, the temperature T_s is defined as the temperature corresponding to the dD/dT maximum. Apparently, T_s shifted to a lower temperature with increasing A_{CH}/A_{OH} value in the range of 0.56 to 1.14, but it remained constant for $A_{CH}/A_{OH}=1.14$ or more. T_s is considered as a rough measure of the glass transition point T_g.

6.4 Discrepancy in some physical properties between conventional and newly prepared cyanoethylated cellulose

If it is assumed that the chemical structure of cyanoethylated cellulose thus

surveyed differs from that of conventional cyanoethylated cellulose as suggested before, then such differences may be reflected in its physical properties. Figure 6-4a shows ***D***-temperature curves for both the sample G and the conventional CEC whose A_{CH}/A_{OH} values are similar, i.e., 1.6 and 1.3, respectively. In the Figure, ***D*** is normalized, i.e., unity at room temperature and zero at the temperature at which the plunger reached the bottom of the glass capillary, indicating completion of liquid flow of the sample. It can be seen that both samples are carbonized above 300°C prior to the melting. However, two diagrams are apparently quite different and the diagram for conventional CEC seems to correspond to what should be obtained for auther's sample with an intermediate degree of cyanoethylation between A and B in Figure 6-3, despite its highly cyanoethylated character.

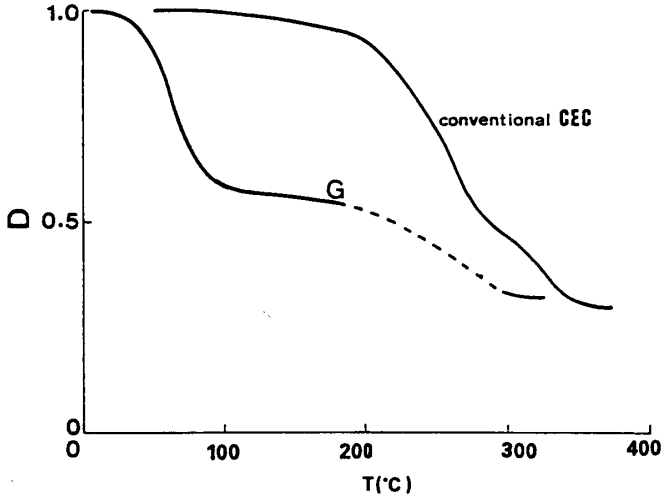

Fig. 6-4a. Diagram of thermal deformation ***D*** versus temperature for both *G* and conventional CEC.

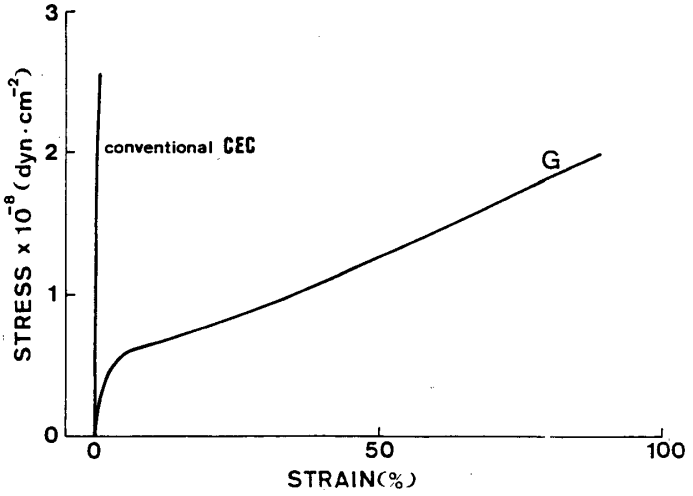

Fig. 6-4b. Stress-strain diagrams for both *G* and conventional CEC in tension measured at room temperature.

Figure 6-4b shows the stress-strain diagrams for both the sample G and conventional CEC in tension measured at room temperature. Regarding conventional CEC, the diagrams is that for brittle polymers. In contrast, for the sample G the diagram shows typical features for tough polymers which result in a flexible film.

6. 5 Comparison of dynamic mechanical properties between conventional and newly prepared cyanoethylated cellulose

From the above differences in physical properties as well as in *DS* mentioned before, cyanoethylated cellulose prepared in PF/DMSO medium can no longr be considered to be the same as conventional cyanoethylated cellulose in chemical structure. However, the difference should be limited to the side chain portion, because these polymers have the same cellulose backbone.

Since the difference in molecular structure in the side chan cause different molecular relaxation mechanism with each other, such differences must be reflected in their viscoelastic properties in the solid state. Figure 6-5 shows the variation of dynamic modulus E', and loss modulus E'' with temperature for both the conventional CEC and the sample G in the range from −190°C to 200°C at 110 Hz. With respect to E'', three relaxation processes were observed for both samples within the experimental frequency and temperature ranges. They are labelled α_{CEC}, β_{CEC}, and γ_{CEC} for the conventional CEC, and α_G, β_G and γ_G for the sample G,

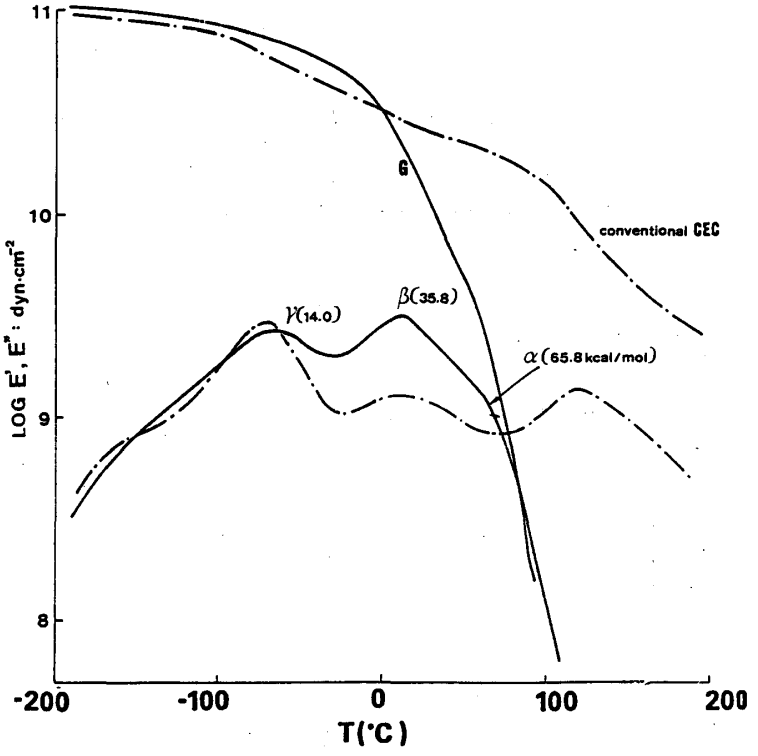

Fig. 6-5. Variation of dynamic modulus E' and loss modulus E'' with temperature for both *G* and conventional CEC at 110 Hz.

respectively, in ordr of decreasing temperature at which they were detected. Noting the conventional CEC first, the drop in E' in the α_{CEC} region was very large. On the other hand, it has been reported that the drop in Young's modulus for highly cyanoethylated cotton yarn at a corresponding temperature region is also very large. This transition is regarded as due to the glass-rubber transition of the sample[57]. Therefore, the α_{CEC} process is considered to result from the short range diffusional motion of the segment along the main chain, i.e., the micro-Brownian motion. In this connection, the chang in $\boldsymbol{D}$ for conventional CEC in this temperature range was too small to be detected as shown in Figure 6-4a.

The γ_{CEC} process is explained with the aid of the results of dielectric measurements for cyanoethylated cellulose after Mikhailov et al.[38]. They reported that the orientational polarization of cyanoethyl groups present in cellulose side chain caused a dielectric relaxation in the temperature and frequency ranges comparable to those for γ_{CEC} process. From this evidence, the γ_{CEC} process can be attributed to the motion involving the cyanoethyl groups of the side chain. The cause of the β_{CEC} remains to be assigned. This process may be ascribed to a kind of complex motion of the conventional CEC and water contained.

Noting the sample G next, both E' and E''-temperature curves were again quite different from those for the conventional CEC as in the other physical properties mentioned above. Concerning E''-temperature curve, both the β_G and γ_G processes revealed a distinct peak, while the α_G process appears as a high temperature shoulder to the β_G peak. On the other hand, the tan δ-temperature plots in the α_G region exhibited a marked peak but those in the β_G and γ_G regions give a shoulder. Hence, the apparent activation energy, ΔE, for the α_G process was determined from tan δ-temperature curves and those for the β_G and γ_G processes were determined from E''-temperature curves. With respect to the α_G process, the maximum value of tan δ exceeds unity and the ΔE value is calculated to be 65.8 kcal/mol, which is of the order of principle dispersions. In addition, the change in value of E' in this region is very large, extending from 5.0×10^9 to 1.3×10^8 dyn/cm^{-2} at temperatures between 60°C and 110°C. From this, the α_G process is considered to be due to the glass-rubber transition. The glass transition temperature of the sample G appeared considerably below that of the conventional CEC. This phenomenon seems itimately related to the molecular mechanism of the β_G process.

The β_G process exhibiting a marked peak in E''-temperature curve induces a remarkable change in E', extending by one order in magnitude in the temperature range between −20°C and 80°C. The ΔE value for the process is calculated to be 35.8 kcal/mol, which is almost of the order of the principle dispersions. These quantities characterizing the β_G proces seem to be unexpectedly large in magnitude,

though they are observed in the glassy state. On the other hand, the temperature frequency locations and maximum E'' value of the γ_G process are similar to those of the γ_{CEC} process. However, suppose that the motion of the cyanoethyl group is responsible for the γ_G process as in γ_{CEC} process, the cause of the β_G process disappears since, in this case, no molecular components in the sample are expected to result in such a process.

6.6 Introduction of oxymethylene groups in the side chain

In the following, an attempt was made to clarify the molecular relaxation mechanism of both the β_G and γ_G processes. In relation to this, the findings in PART II for the acetylated cellulose prepared by acetylation in PF/DMSO medium are worth reviewing. This acetylated cellulose is called cellulose oligo-oxymethylene ether acetate, CAcOM, whose chemical structure is different from conventional acetylated cellulose in that oxymethylene oligomer is introduced at the position between glucopyranose ring and acetyl group. The introduction of oxymethylene oligomer results from dissolving cellulose in PF/DMSO medium in which cellulose is dissolved as cellulose hydroxy oligo-oxymethylene ether. For CAcOM, two relaxation processes were observed in the glassy state. One stems from micro-Brownian motion along the side chain independent of the micro-Brownian motion along the main chain, resulting in a large relaxation such as the β_G process. The other arises from the motion of the intervening oxymethylene group between glucopyranose ring and acetyl group, and it appears in the vicinity of the γ_G process. I should be noted that since the sample G is also obtained by the reaction of cellulose in PF/DMSO medium, it is most probable that the side chain of the sample G is not composed of cyanoethyl group, but instead, it consists of $-(CH_2O)_n-CH_2-CH_2-CN$ group. If this is the case, the micro-Brownian motion along the side chain as in CAcOM is responsible for the β_G process in the sample G.

However, cyanoethylation of cellulose oligo-oxymethylene ether in the presence of slight amount of strong basic catalyst such as NaOH or NaH results in rapid elimination of hydroxy oligo-oxymethylene side group because of its unstable hemiacetal structure. Therefore, it is necessary to clarify whether or not the introduced hydroxy oligo-oxymethylene group in the side chain is removed when Na/DMSO is used as a catalyst. Figure 6-6 shows E'' versus temperature curves at 110 Hz for the sample B, acetylated B and CAcOM below room temperature. For the sample B, a large relaxation process at around -50°C is observed, and the process can be attributed to the motion of methylol group in a similar manner as that in cellulose, since the sample B was not cyanoethylated to a great extent as shown in Figure 6-1. On the other hand, for the acetylated B the relaxation

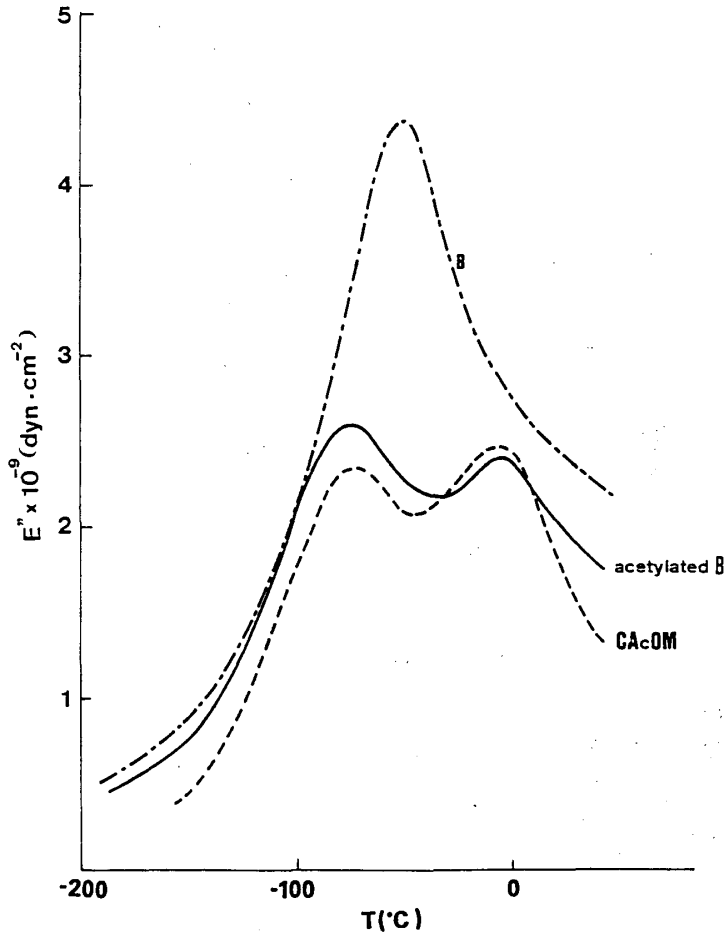

Fig. 6-6. Variation of loss modulus E'' with temperature for *B*, acetylated *B* and CAcOM at 110 Hz. Acetylated *B* was prepared by acetylation in the reaction mixture which gave *B* when it was poured into excess methanol.

process due to $-CH_2OH$ motion disappears, and instead, two other processes appear at around −75°C and −5°C, respectively. It should be noted that these two processes correspond closely to those for CAcOM. In addition, the thermodiagram for acetylated B is also similar to that for CAcOM. Therefore, the acetylated B is regarded as almost the same as CAcOM, indicating that the process in higher temperatures is due to the micro-Brownian motion of the side chain and the process in lower temperature is due to the motion of oxymethylene groups which is located in the position between glucopyranose ring and acetyl groups. From these findings, it was concluded that the formation of hydroxy oligo-oxymethylene group in PF/DMSO was little affected even if basic catalyst, Na/DMSO, is added to the system.

6.7 Molecular origin of the β_G and γ_G processes

It is not yet clear whether or not oxymethylene oligomer is introduced at the

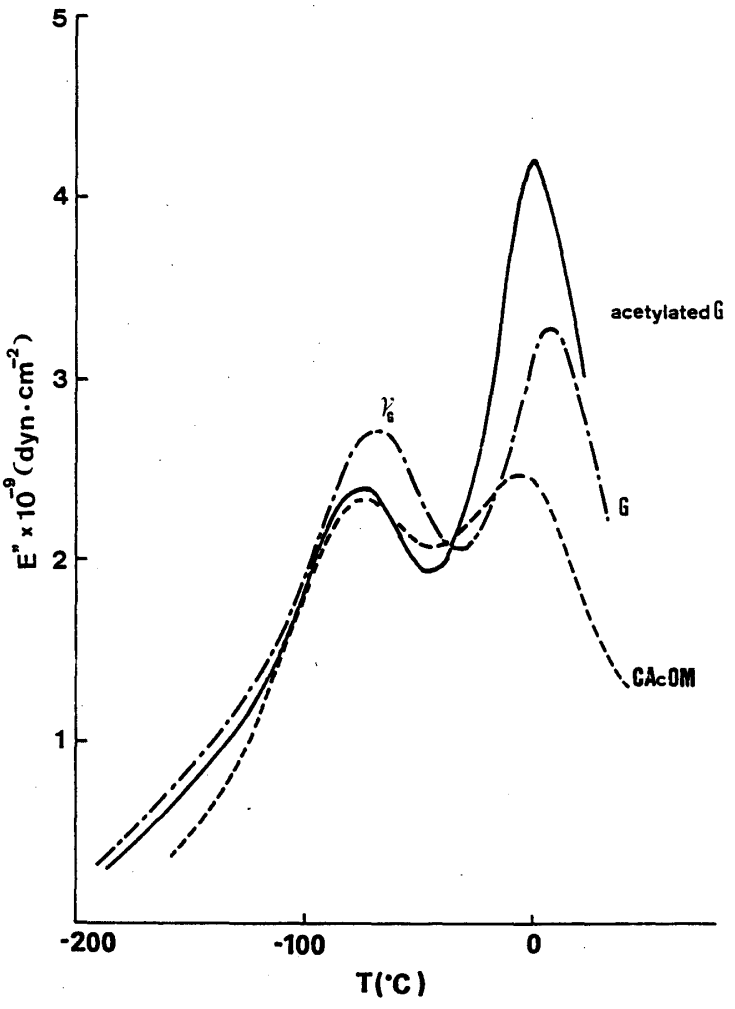

Fig. 6-7. Variation of loss modulus E'' with temperature for *G*. acetylated *G* and CAcOM at 110 Hz. Acetylated *G* was prepared by acetylation in the reaction mixture which gave *G* when it was poured into excess methanol.

intermediate position between glucopyranose ring and cyanoethyl groups. For the purpose of elucidating this point, E''-temperature curves at 110 Hz for the sample G, acetylated G and CAcOM are compared in Figure 6-7. For the sample G, the γ_G process may includes the motion of methylol groups because the absorption band due to OH groups still remains in its infrared spectrum (Fig. 6-1). On the other hand, for the acetylated G the γ_G process shifts somewhat to a lower temperature region, decreasing in height, but it still remains despite the absence of methylol groups. This slight change of the γ_G process can be considered to be due to the extinction of the contribution of CH_2OH motion to the γ_G process. It is of interest to note that the γ_G process in acetylated G corresponds closely to the process in CAcOM which is due to the motion of oxymethylene groups between glucopyranose ring and acetyl groups. However, acetyl contents in acetylated G is

small because acetylated G is highly cyanoethylated prior to acetylation. Therefore, if the oxymethylene groups are responsible for the γ_G process, they are required to be situated in the position between glucopyranose ring and cyanoethyl groups as well as between glucopyranose ring and acetyl groups. From these reasonings, it is most probable that the γ_G process in the sample G is ascribed to the motion initiated by oxymethylene groups in the side chain in addition to methylol groups. If such is the case, the micro-Brownian motion along the side chain (which consists of $-(CH_2O)_n-CH_2-CH_2-CN$) is considered to cause the β_G process showing marked relaxation with a large ΔE value. In this connection, the release of micro-Brownian motion along, the side chain induces a weakening of interchain cohesive force, facilitating chain backbone motion to lower the temperature region of the α_G process, as compared with that of α_{CEC} process.

6.8 Reconsideration of the infrared spectra of newly prepared cyanoethylated cellulose

With above considerations in mind, one should again investigate infrared spectra of the sample G. Figure 6-8 shows infrared spectra of the sample G, conventional CEC and cyanoethylated xylan prepared in PF/DMSO medium. For

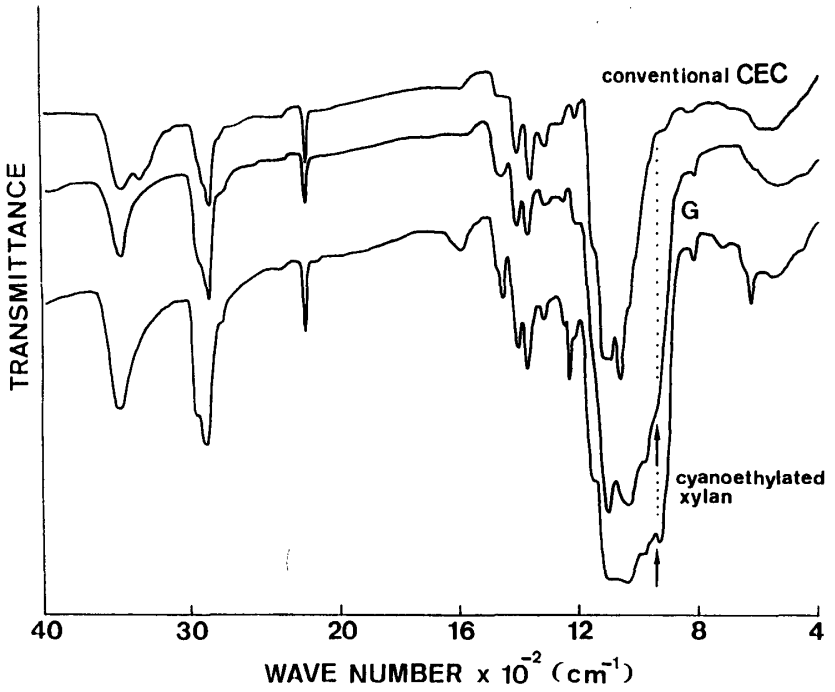

Fig. 6-8. Infrared spectra of conventional CEC, *G*, and cyanoethylated xylan. Cyanoethylated xylan was prepared from birch xylan supplied from Aldrich Co. The preparation procedure is almost the same as that for *G*. But, in this case, dissolution time of xylan in PF/DMSO is about 31 min. 50 min shorter than for *G*.

conventional CEC, no absorption was observed at around 950 cm^{-1}. In contrast, the spectrum of the cyanoethylated xylan exhibit a distinct absorption at about 950 cm^{-1}. By noting these two spectra, it is clear that the spectrum of the sample G reveals absorption at the same band. On the other hand, it has been reported that the absorption band due to stretching vibration of methylene dioxy groups[58] appears at about 950 cm^{-1}. Consequently, it is concluded that the sample G has oxymethylene groups in the side chain as expected before, and thus cyanoethylated cellulose prepared in PF/DMSO medium is regarded as a novel cellulosic material.

6.9 Estimation of *DS* values

It is worthy to remember, here, that the *DS* values of conventional CEC and sample G were calculated to be 2.3 and 1.3, respectively, though they seem similar in *DS* from their infrared spectra. The cause of this discrepancy stemms from taking no account of differences in chemical structure between the sample G and conventional CEC, when their *%N* values are converted to the *DS* values. Therefore, the conversion formula usually used for cyanoethylated cellulose such as conventional CEC should be rewritten for the sample G, considering the introduction of $-(CH_2O)_n-$ groups in the side chain. The result is expressed as follows;

$$DS=(162\times\%N)/(1400+\%N-(54+30n)\times\%N),$$

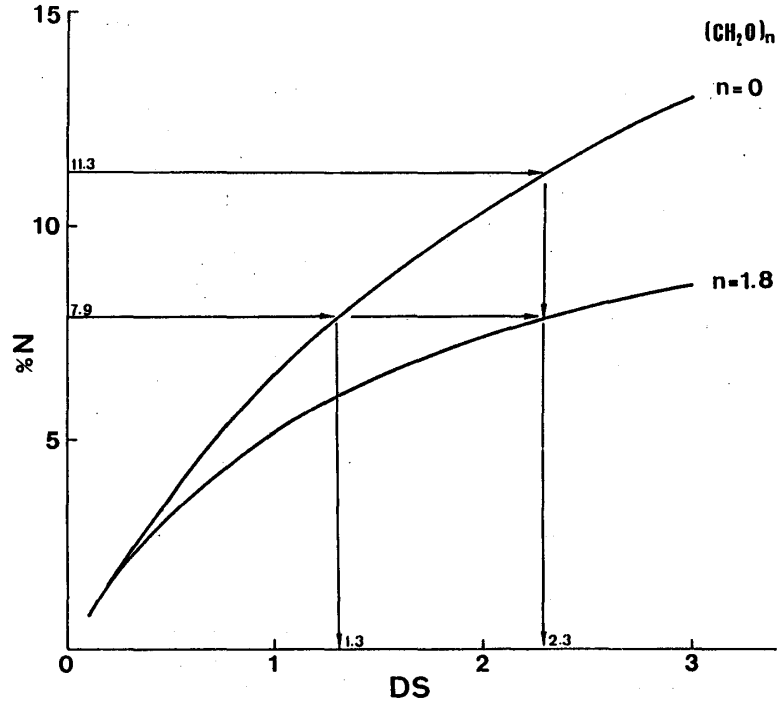

Fig. 6-9. Conversion diagrams of percentage of nitrogen contents (*%N*) to *DS* value for cyanoethylated cellulose with and without oxymethylene groups $-(CH_2)_n-$ in the side chain.

where n is determined as 1.8 from the corresponding NMR intergral for CAcOM. In case of $n=0$, the formula agrees with conventional conversion formula for cyanoethylated cellulose. Figure 6-9 shows the relation between $\%N$ and DS for cyanoethylated cellulose whose n values are 0 and 1.8, respectively. From the figure, it is found that $\%N$ of 11.3 for conventional CEC and 7.9 on the curve in Figure 6-2 correspond to the same DS value of 2.3, when they are calculated from respective conversion formula. In the same manner, the DS value of the sample G with $\%N=8.3$ is estimated to be about 2.5.

Further evidence for DS value of the sample G is given in Figure 6-10 by the comparison of infrared spectra of the sample G, acetylated G and CAcOM with $DS=0.5$. For the acetylated G, it is clear that there was little absorption band due to residual OH groups, while the absorption band due to C=O groups at 1,350 cm^{-1} is recognized. It should be emphasized that when the absorption ratio of A_{1750}/A_{1100} is adopted as a measure of the degree of acetylation, the value of A_{1750}/A_{1100} for the acetylated G is similar to that of CAcOM with $DS=0.5$. Therefore, it is concluded that the DS of the sample G is ca. 2.5.

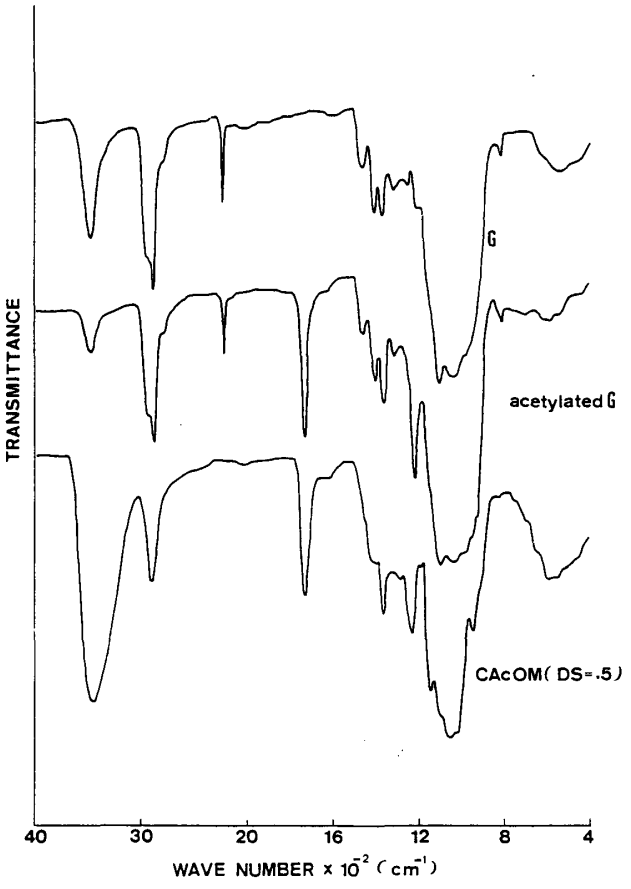

Fig. 6-10. Infrared spectra of G, acetylated G, and CAcOM with $DS=0.5$.

Conclusion

For the future increase in the use of cellulose derivatives as plastic materials, the auther intended to clarify fundamental features of their physical properties, especially viscoelastic properties. The samples used were cellulose acylates series, COAs series, and novel cyanoethylated cellulose. These polymers have a common feature in that the motional unt of the main chain is bulky glucopyranose ring while that of the side chain mainly involves small size group such as methylene unit. Such a structure is substantially different from that of usual synthetic polymers. From this, cellulose derivatives examined were expected to show unique relaxation phenomenon as compared with those in synthetic polymers.

Regarding cellulose acylates series, five kinds of mechanical relaxation process (α_m, β_m, β'_m, γ_m, and γ'_m processes) and four kinds of dielectric processes (α_d, β_d, γ_d, and γ'_d processes) were detected within the frequency and temperature ranges examined. They were attributed, respectively, to the micro-Brownian motion of the main chain (α_m, α_d), the motion of the side chain (β_m, β'_m), motion of oxycarbonyl group (β_d), motion of three or more methylene groups (γ_m, γ_d), and motion of two methylene groups (γ'_m, γ'_d). Since the dielectrically active oxycarbonyl group in the side chain is bonded directly to the glucopyranose ring, its orientational polarization (β_d) did not reflect the side chain motion (β_m), although other processes with the same Greek letters were similar in molecular mechanism. For the higher homologue with linear acyl side chain, unexpectedly large relaxation was observed in the region of the β_m process. The side chain motion responsible for the β_m process was considered to shift from the hindered rotation or the twisting to the micro-Brownian motion of the side chain with increasing the side chain length.

The COAs are different in chemical structure from the above cellulose acylates in that the oligo-oxymethylene groups are bonded between glucopyranose ring and acyl side group. With respect to COAs series, four kinds of mechanical relaxation process (α, β, γ, δ and δ') were detected in the range similar to that employed for cellulose acylates. These α and δ' processes were, respectively, attributed to the micro-Brownian motion of the main chain (α), motion of the side chain (β), motion of oligo-oxymethylene group (γ), motion of three or more methylene groups (δ), and motion of two methylene groups (δ'). In contrast to cellulose acylates series, the β relaxation was very large in magnitude even for the acetate in COAs. The activation energy and activation entropy for the β process in all COAs were calculated to be ca. 30 kcal/mol and 100 eu, respectively. The process was thought to be due to the micro-Brownian motion in the side chain as was observed in cellulose acylates with long acyl side chain. The occurence of such motion for COAs with short acyl side chain was explained by considering the role of oxymethylene

group in the side chain. From the above results, it was concluded that both cellulose acylates and COAs are characterized by observing that the micro-Brownian motion in the side chain appears separately from that of the main chain. In this connection, with increasing acyl side chain length, the difference in viscoelastic properties between cellulose acylates and COAs became negligibly small because the β'_m loss peak in cellulose acylates and γ loss peak in COAs become to merge into the dominant β_m and β peaks, respectively. Although the presence of the β process is characteristic for all COAs with linear side chain, it was also possible to eliminate the β process by introducing bulky group such as glucopyranose ring in the side chain.

On the basis of the above results, the auther finally examined chemical structure and physical properties of cyanoethylated celluloe prepared by the reaction in PF/DMSO medium. This cyanoethylated cellulose was found to be a novel cellulose derivatives, which includes oligo-oxymethylene groups at the position between glucopyranose ring and cyanoethyl group in the side chain. The new polymer exhibited the micro-Brownian motion in the side chain as well as that of the main chain as in cellulose acylates or in COAs. Also, it gave clear, transparent films which suggests the posibility of being applicable to various new fields.

Acknowledgments

The auther is deeply grateful to professor Tadashi Yamada, Wood Research Institute, Kyoto University, for his instruction and encouragement during the entire course of this study.

The auther also wishes to express his sincerest thanks to Professor Nobuo Shiraishi and Professor Kouji Murakami, Department of Wood Science and technology, Faculty of Agriculture, Kyoto University, for their helpful suggestions and critical readings of the manuscript.

Special thanks are also due to Associate Professor Misato Norimoto, Wood Research Institute, Kyoto University, and Professor Keizo Okamura, Department of Wood Science and Technology, Faculty of Agriculture, Kyoto University, for their profitable advice and the kindest support in the various phases of this study.

It is great pleasure to acknowledge the hospitality and encouragement of Mr. Takaya Nomura, and other members of Research Section of Wood Physics, Wood Research Institute, Kyoto University.

Referencess

1) S.M. HUDSON and J.A. CUCULO: J. Macromol. Sci., **C18**, 1 (1980).
2) K. MATSUZAKI and K. UDA: Sen-i Gakkaishi, **38**, P-156 (1982).
3) T.P. NEVELL and S.H. ZERONIAN: Cellulose Chemistry and Its Application, John Wiley

& Sons, New York, USA, Chapter 7 (1985).
4) C.L. MacCormick and D.K. Lichatowich: J. Polymer Sci., Polymer Letter Ed., **17**, 479 (1979).
5) D.L. Johnson: US Patent, 3,508, 941 (1970).
6) W.F. Fowler Jr, C.C. Unruh, P.A. McGee and W.O. Kenyon: J. Amer. Chem. Soc., **69**, 1636 (1947).
7) D.L. Johnson, M.D. Nicholson and F.C. Haigh: Applied Polymer Symposia, No. 28, Part 3, 931 (1976).
8) K. Hata and K. Yokota: Sen-i Gakkaishi, **22**, 96 (1966).
9) K. Hata and K. Yokota: Sen-i Gakkaishi, **24**, 415 (1968).
10) O. Nakao: Sen-i to Kogyo, **4**, No. 3, 128 (1971).
11) R.G. Schweiger: Carbohydr. Res., **70**, 185 (1979).
12) D.L. Johnson: US Patent, 3,447, 939 (1969).
13) A. Ishizu: The Sixth Conference on High Polymers, Osaka, Japan, P79 (1983).
14) A. Isogai, A. Ishizu and J. Nakano: J. Applied Polymer Sci., **29**, 2097 (1984).
15) M.D. Nicholson and D.C. Johnson: Cell. Chem. Technol., **11**, 349 (1977).
16) N. Shiraishi, Y. Miyagi, S. Yamashita, T. Yokota and Y. Hayashi: Sen-i Gakkaishi, **35**, 466 (1979).
17) N. Shiraishi, T. Katayama and T. Yokota: Cell. Chem. Technol., **12**, 429 (1978).
18) R.B. Seymour and E.L. Johnson: J. Polymer Sci., Polymer Chem. Ed. **16**, 1 (1978).
19) J.M. Tedder: Chemical Review, **55**, 787 (1955).
20) H.S. Sack, T.R. Cuykendall and T.J. Wood: Physical Review, **94**, 1414 (1954).
21) K. Nakamura: Kobunshi-Kagaku, **13**, 47 (1956).
22) J. Russel and R.G. Van Kerpel: J. Polymer Sci., **25**, 77 (1957).
23) R.W. Seymour, S. Weinhold and S.K. Heynes: J. Macromol. Sci. Phys., **B16**, 337 (1979).
24) A.F. Klarman, A.V. Galanti and L.H. Sperling, J. Polymer Sci. A-2, **7**, 1513 (1969).
25) T. Morooka, M. Norimoto, T. Yamada and N. Shiraishi: Wood Research, No. 69, 61 (1983).
26) M. Tuzuki, N. Shiraishi and T. Yokota: J. Applied Polymer Sci., **25**, 2567 (1980).
27) S.S. Roger and L. Mandelkern: J. Physical Chem., **61**, 958 (1957).
28) R.E. Boy, R.M. Schulken Jr. and J.W. Tamblyn: J. Applied Polymer Sci., **11**, 2453 (1967).
29) N.G. MacCrum, B.E. Read and G. Williams: Anelastic and Dielectric Effects in Polymeric Solids, John Willey & Sons, London, UK (1967).
30) J. Kolarik: Adv. Polymer Sci., **46**, 119 (1982).
31) G.P. Mikhailov and T.I. Borisova: Sov. Phys. Tech. Phys., **3**, 120 (1958).
32) T. Morooka, M. Norimoto, T. Yamada and N. Shiraishi: J. Applied Polymer Sci., **29**, 3981 (1984).
33) C.J. Malm, J.W. Mench, D.L. Kendall and G.D. Hiatt: Ind. Eng. Chem., **43**, 684 (1951).
34) G.P. Mikhailov, A.I. Artyukov and V.A. Shevelev: Polymer Sci. USSR, **11**, 628 (1969).
35) D.J. Crofton, D.M. Moncrieff and R.A. Pethrick: Polymer, **23**, 1605 (1982).
36) S. Saito and T. Nakajima: Bull. Electrotech. Lab., **22**, 654 (1958).
37) N. Kato, H. Saito, S. Yabumoto and R. Fujishige: Kobunshi-kagaku, **19**, 95 (1962).
38) G.P. Mikhailov, A.I. Artyukov and T.I. Borisova: Polymer Sci. USSR, **9**, 2713 (1967).
39) T. Morooka, M. Norimoto and T. Yamada: Wood Recuarch, No. 70, 29 (1984).
40) T.J. Baker, L.R. Schroeder and D.C. Johnson: Carbohydr. Res., **67**, C4 (1976).
41) T. Morooka, M. Norimoto, T. Yamada and N. Shiraishi: J. Applied Polymer Sci., **27**, 4409 (1982).
42) L.E. Nielsen: Mechanical Properties of Polymers and Composites, Marcel Dekker, New York, USA (1974).
43) A.H. Willbourn: Trans. Faraday Soc., **54**, 717 (1958).

44) E.A.W. HOFF, D.W. ROBINSON and A.H. WILLBOURN: J. Polymer Sci., **18**, 161 (1955).
45) J.D. FERRY, W.C. CHILD, R. JAND, D.M. STERN, M.L. WILLIAMS and R.F. LANDEL: J. Colloid Sci., **12**, 53 (1957).
46) Y. MIYAGI, N. SHIRAISHI, T. YOKOTA, S. YAMASHITA and Y. HAYASHI: J. Wood Chem. Technol., **3**, No. 1, 59 (1983).
47) T. MOROOKA, M. NORIMOTO, T. YAMADA and N. SHIRAISHI: Wood Research, No. 72, 12 (1986).
48) T. MOROOKA, M. NORIMOTO, T. YAMADA, S. TAKUMA and K. OKAMURA: J. Applied Polymer Sci., in press.
49) T. AOKI: Wood Research Technical Note, No. 15, 61 (1980).
50) J. KOLARIK, K. MURTINGER and S. SEVIK: J. Applied Polymer Sci. Phys., **22**, 773 (1984).
51) M. NORIMOTO, T. MOROOKA, T. AOKI, N. SHIRAISHI, T. YAMADA and F. TANAKA: Wood Research Technical Note, No. 17, 181 (1983).
52) J.H. MACGREGOR: J. Soc. Dyers and Colourists, **67**, 66 (1951).
53) N.M. BIKALES and L. SEGAL: Cellulose and Cellulose Derivative, Part 3, John Wiley & Sons, New York, USA (1971).
54) A.J. HALL: Text. Merc., **130**, 103 (1954).
55) T. MOROOKA, M. NORIMOTO and T. YAMADA: J. Applied Polymer Sci., **32**, 3575 (1986).
56) L. BROWN, P. HOLLIDAY and I.F. TROTTER: J. Chem. Soc., 1532 (1951).
57) C.M. CONRAD, D.J. STANONIS, P. HARBRINK and J.J. CREELY: Text. Res. J., **30**, 339 (1960).
58) L.H. BRIGGS, L.D. COLEBROOK, H.M. FALES and W.C. WILDMAN: Anal. Chem., **29**, 904 (1957).